AEDC-TR-70-287



# EVALUATION OF A PRESSURE GAGE ROTATING IN A MOLECULAR FLUX

J. D. Haygood and R. Dawbarn

ARO, Inc.

April 1971



**VON KÁRMÁN GAS DYNAMICS FACILITY**
**ARNOLD ENGINEERING DEVELOPMENT CENTER**
**AIR FORCE SYSTEMS COMMAND**
**ARNOLD AIR FORCE STATION, TENNESSEE**

# NOTICES

# EVALUATION OF A PRESSURE GAGE ROTATING IN A MOLECULAR FLUX

J. D. Haygood and R. Dawbarn
ARO, Inc.

## FOREWORD

The research presented in this report was sponsored by the Air Force Cambridge Research Laboratory (AFCRL), Air Force Systems Command (AFSC), under Program Element 61102F, Project 8605.

The results of the work were obtained by ARO, Inc. (a subsidiary of Sverdrup & Parcel and Associates, Inc.), contract operator of the Arnold Engineering Development Center (AEDC), AFSC, under Contract F40600-71-C-0002. The work was performed in the period from July 1, 1969, to June 1970 under ARO Project No. SW5010, and the manuscript was submitted for publication on September 29, 1970.

This technical report has been reviewed and is approved.

William G. Moretti, Jr.
Major, USAF
Research and Development
Division
Directorate of Technology

Harry L. Maynard
Colonel, USAF
Director of Technology

## ABSTRACT

The purpose of this project was to help evaluate data obtained from an ion gage flown on board the OV1-15 satellite. The aerodynamic molecular beam facility was modified to produce a molecular beam with a 5-in.-diam test core. This system was used to determine the effects of a changing angle of attack on the pressure reading in a hot cathode magnetron ionization gage. Static calibrations were made for various orientations of the gage to the beam flow. Dynamic calibrations were made with the gage rotating in the beam flow at approximately 2 rpm. A comparison of static and dynamic profiles showed no detectable differences, thus indicating negligible sorption effects within the gage. The sensitivity factor for the gage was determined by calibrating the gage in a vacuum system where the random gas pressure could be controlled and set at known values. A matrix of correction factors was prepared which may be used to adjust the observed gage reading at a known attitude and azimuth angle to that pressure which would have been observed with the same molecular flux and the gage at 0-deg attitude and 0-deg azimuth.

# CONTENTS

| | | Page |
|---|---|---|
| | ABSTRACT | iii |
| I. | INTRODUCTION | 1 |
| II. | APPARATUS | 2 |
| III. | EXPERIMENTAL PROCEDURES | 3 |
| IV. | RESULTS | 8 |
| V. | CONCLUSIONS | 11 |
| | REFERENCES | 11 |

## TABLE

| | | |
|---|---|---|
| I. | Test Schedule | 5 |

## APPENDIX
### Illustrations

| Figure | | |
|---|---|---|
| 1. | OV1-15 Satellite | 15 |
| 2. | View of Gage Entrance | 16 |
| 3. | Schematic of Molecular Beam Chamber | 17 |
| 4. | View of Gage Movement Mechanism | 18 |
| 5. | Schematic of Gage Calibration Chamber | 19 |
| 6. | Molecular Beam Profile | 20 |
| 7. | View of Microwave Cavity | 21 |
| 8. | Sample of Density Signal Output during One Rotation | 22 |
| 9. | Data from GE Gage | 23 |
| 10. | Data from CRL Gage | 36 |
| 11. | Matrix of Correction Factors | 51 |
| 12. | Pressure Profile for Constant Azimuth | 52 |
| 13. | Pressure Profile for Constant Attitude | 53 |
| 14. | Pressure Profile for Varying Azimuth and Attitude | 54 |
| 15. | Schematic of CRL Gage | 55 |
| 16. | Predicted Pressure Profiles | 56 |
| 17. | Satellite Data Indicating Oscillations | 61 |

# SECTION I
# INTRODUCTION

The purpose of this project was to help evaluate data obtained from an ion gage flown on board the OV1-15 satellite. The OV1-15 experiments were to determine the cause of the large and sudden fluctuations observed in Air Force satellite trajectories, with the ultimate goal of being able to predict the occurrence and magnitude of such fluctuations. The CRL ion gage was one of the experimental packages on board and was used to measure atmospheric density. The gage as mounted in the satellite is shown in Fig. 1, Appendix. Once in orbit the satellite was spin-stabilized and rotated about the axis noted in Fig. 1. Subsequent ground-based observations indicated that the spin axis was not normal to the flight vector. Thus the resulting precession of the spin axis about the flight vector lead to a complex variation in aspect angle or angle of attack of the pressure gage to the gas flux. Had the satellite been inserted in orbit as planned, each revolution of the satellite would have yielded one data point where the gage was looking directly ahead into the flow stream. Since the spin rate was sufficiently rapid these data points would have been adequate to map the atmospheric density without large discontinuities. However, because of the complex motion of the gage on the actual flight there were long periods of time when the gage did not look directly ahead but only reached a minimum aspect angle before regressing. It was therefore necessary to find a suitable correction factor which could be applied to the pressure readings transmitted by the pressure gage which would correct for the angle of attack. A theoretical paper prepared by Hughes at the University of Toronto (Ref. 1) provides a basis for calculating this correction factor. His analysis considers a tubulated gage immersed in a flow field. An equilibrium pressure in the gage will be reached when the rate of flow of molecules into the gage equals the rate of molecules flowing out. Since these two rates are influenced by the dimensions and angle of attack of the tubulation, the problem becomes one of predicting the effects of directed versus random flow down tubes. Several assumptions are made in the analysis. Included among these assumptions are that:

1. The flows are free molecular and thus the incoming flux does not interact with the exiting flux.

2. The gage volume is large compared to the dimensions of the tube.

3. The directed flow accommodates to the tubulation temperature upon first impact and is subsequently reflected with a cosine distribution.

4. There is no outgassing or sorption in the gage (i.e., no sources or sinks)

5. The entrance to the gage is a well-defined circular tube.

For the satellite gage, assumptions (1) and (2) are valid. Assumption (3) is questionable because of evidences of specular reflections by high energy molecules from engineering surfaces (Ref. 2). Assumption (4) is also suspect because the gage is constructed of titanium and ceramic and numerous investigators have reported on the sorption of nitrogen by titanium. The fifth assumption is obviously invalid since the gage entrance is not a circular tube but consists of ion deflection plates and a cap opening device (Fig. 2).

In order to evaluate the operation of this gage when rotating in a molecular flow field, the following tests were defined. The objective was to provide a molecular flux which would simulate the density range in the upper atmosphere and mount the gage in a suitable mechanism so that it could be rotated to simulate the motions of the satellite.

The test program was divided into four phases:

1. Produce a molecular beam having a speed ratio of S = 10 with a uniform test core approximately 5 in. in diameter.

2. Build a suitable gage movement mechanism and evaluate its performance with a dummy glass envelope gage.

3. Install the CRL test gage and obtain data consisting of gage reading as a function of aspect angle for both dynamic and static conditions.

4. Calibrate the CRL test gage in a vacuum chamber with random gas influx.

# SECTION II
# APPARATUS

The tests were conducted in two test cells: the Aerodynamic Molecular Beam Chamber and the 2- x 3-ft Research Vacuum Chamber.

The Aerodynamic Molecular Beam Chamber is shown in Fig. 3 and described in Ref. 3. It was modified for these test by substituting a cryogenically cooled skimmer with a 1-in. orifice for the nominal 4-mm conical skimmer and enlarging the collimating orifice from its nominal 8-mm diameter to 4-in. diameter. These changes produced a molecular beam with a useable test core of approximately 5 in. A small ionization gage with the opening reduced to a 4-mm-diam orifice was mounted on a remotely controlled traverse and used to map the flow field through the test core of the beam. The gas source, which is normally a resistance-heated tube, was replaced with a tuneable microwave cavity with a thin-walled orifice. The cavity operated as the gas plenum, and the aerodynamic beam was skimmed from the gas jet as it expanded from the thin-wall orifice.

## 2.1 GAGE MOUNTING SYSTEM

The test gage was mounted in a specially prepared movement mechanism shown in Fig. 4. The front face of the cannister enclosure was built to conform as closely as possible to the hardware that surrounded the flight gage on the satellite. This cannister was then suitably counterbalanced and pivoted so that it could be rotated in both the horizontal and vertical planes. The pivot point chosen was in the center of the gage opening. This assured that regardless of the aspect angle the gage opening stayed in a region of constant molecular flux. Two gear-head motors were installed to operate the pivot mechanisms. Potentiometers coupled to the pivot shafts were used to provide a remote readout of the gage orientation.

## 2.2 CALIBRATION CHAMBER

Sensitivity calibrations of the test gage were conducted in the vacuum system shown in Fig. 5. This chamber is used for gage calibration and gage comparison studies. It is equipped with a calibrated gas addition system. A full description of the chamber and methods of gage calibration may be found in Ref. 4.

# SECTION III
# EXPERIMENTAL PROCEDURES

## 3.1 PRODUCTION OF MOLECULAR BEAM

The present state of the art precludes providing a molecular beam of sufficient intensity with velocities of 8 km/sec and static temperatures of approximately 1500°K (speed ratio (S) = 10). However, since the purpose of the test series was to measure the effect of angle of attack on the pressure gage reading and theoretical analysis indicates that this is a function of the speed ratio, the beam conditions were tailored to provide the appropriate molecular flux with a lower velocity and static temperature which still produced a speed ratio of 10. Previous calibrations of molecular beams in this facility (Ref. 5) using time-of-flight techniques to determine molecular velocities and velocity distributions were used to define the required source conditions. For nitrogen gas a source pressure of 13 mm of mercury (Hg) and a temperature of 300°K was used. The expanding gas from this source was skimmed by a 20°K gaseous-helium (GHe)-cooled donut. The core which passed through the center of the donut was further collimated by a 4-in. orifice located 18 in. downstream. The profile of the resulting beam is shown in Fig. 6. These data have been normalized to the maximum pressure recorded by the small orifice probe used to survey the beam ($2.1 \times 10^{-5}$ torr). Because of the large cross section of the beam and the resulting quantity of gas, the background pressure in the test section of the cell rose from its normal $5 \times 10^{-8}$ torr to $7 \times 10^{-7}$ torr.

Since a possible perturbation of satellite data could have been produced by atomic oxygen in the upper atmosphere, an attempt was made to produce a beam which consisted of molecular and atomic oxygen. The microwave cavity which served as a gas source plenum is shown in Fig. 7. The system was installed in the test section and a beam of oxygen was produced. Comparisons of the spectra taken with the microwave cavity on and with it off produced results which were inconclusive. The increased noise levels of spectra taken with the cavity on, plus a slowly declining sensitivity of the mass spectrometer attributable to the oxygen, masked the increase, if any, in the mass 16 peak.

## 3.2 INSTALLATION OF MOVEMENT MECHANISM AND CHECKOUT

As previously noted, the movement mechanism was constructed to duplicate as near as possible the surrounding hardware of the flight gage installed in the satellite.

In order to evaluate the movement mechanisms under vacuum conditions and, even more, to investigate possible noise induced into gage readings because of the operation of the DC drive motors, a small glass envelope gage was fitted with an entrance aperture to approximate the CRL gage and mounted in the system. A series of test runs was made with this system, and several modifications in gearing and electrical lead routings were made. Data from these runs in the form of pressure reading versus aspect angle were recorded.

### 3.3 INSTALLATION AND TEST OF CRL GAGE

The CRL gage was installed in the movement mechanism and its electronics package located on a shelf inside the vacuum system. Outputs from the electronics package were brought out of the vacuum system and connected to a strip-chart recorder. The recommended electrial checkout procedure for the CRL gage was conducted before the cell was closed up and evacuated (Ref. 6).

When the cell had reached test conditions ($3 \times 10^{-8}$ torr) the remote movement mechanism was operated to ensure that no cables were binding. At this point 28 v was applied to the explosive squibs which were to deploy the gage cap. Neither squib fired with the 28-v supply. A tesla coil was connected in parallel with the supply and both squibs fired and deployed the cap. The power supply to the CRL gage was turned on and the filament inside the gage heated up, but there was no gage output. Electrical checks indicated that there was a short circuit in the 300-v anode supply somewhere inside the cell. Attempts to relieve the short by manipulating the gage movement mechanism were unsuccessful. The cell was returned to atmospheric pressure with argon. A purge of argon was kept on the CRL gage while the electrical short was traced. No definite short circuit was located since during the continuity checks the short disappeared. However numerous small cuts were observed in the rubber insulation covering the high voltage lead. A new wiring harness was made using Teflon®-covered wire and the electronics package was removed from inside the vacuum cell and relocated outside. The cell was again closed and returned to test conditions. During the electrical checkout procedure of the gage it was noted that the gage sensitivity was lower than normal. This was traced to below-nominal voltages supplied by the electronics package. Since an examination of the electronics indicated that it was not feasible to correct the problem in the test time available, and it was decided that the loss in sensitivity would not seriously impair the results of the test, a record of the actual operating voltages was made and the test schedule was started.

The test sequence consisted of establishing the molecular beam and checking its intensity with the chamber instrumentation (survey ion gage probe). The CRL gage was then adjusted to zero azimuth and rotated stepwise through 360-deg attitude. At each step the gage was stopped and allowed to come to equilibrium.

The next tests were dynamic and consisted of remotely setting the gage movement mechanism to a specific azimuth angle and then rotating the gage through ±360-deg attitude at approximately 2 rpm. The gage output was recorded continuously during this rotational period. Azimuth angles were varied from -40 to 80 deg in 10-deg intervals. One sample of data for 0-deg attitude was recorded on a strip chart and is reproduced in Fig. 8. A complete record of the test schedule is reproduced in Table I.

**TABLE I**
**TEST SCHEDULE**

| Run | Time | Forepressure | Gas | Azimuth,deg | Comments |
|---|---|---|---|---|---|
| 1 | 8:55 | 19 | $N_2$ | 0 | Static Tests -180 to 180 deg |
| 2 | 9:05 | | | 0 | Dynamic Tests 4 cycles |
| 3 | 9:08 | | | 10 | Dynamic Tests 4 cycles |
| 4 | 9:25 | | | 20 | Dynamic Tests 2 cycles |
| 5 | 9:27 | | | 30 | |
| 6 | 9:32 | | | 40 | |
| 7 | 9:35 | | | 50 | |
| 8 | 9:38 | | | 60 | |
| 9 | 9:41 | | | 70 | |
| 10 | 9:42 | | | 80 | |
| 11 | 9:45 | | | -10 | 16.2 sec/revolution |
| 12 | 9:48 | | | -20 | |
| 13 | 9:50 | | | -30 | |
| 14 | 9:52 | | | -40 | |
| 15 | 10:11 | 15 | | 0 | GE gage $1 \times 10^{-5}/2 \times 10^{-7}$ |
| 16 | 10:22 | 10 | | 0 | GE gage $5.8 \times 10^{-6}/1.4 \times 10^{-7}$ |
| 17 | 10:50 | 20 | Ar | 0 | 4 cycles GE gage $3.7 \times 10^{-5}/$ $4.6 \times 10^{-7}$ |
| 18 | 11:13 | 10.5 | $O_2$ | 0 | 4 cycles GE gage $5.5 \times 10^{-6}/$ $1.5 \times 10^{-7}$ |
| 19 | 11:24 | 10.5 | O | 0 | microwave on (no cooling water) GE gage $5.5 \times 10^{-6}/$ $1.5 \times 10^{-7}$ |
| 20 | 11:45 | 18.7 | $N_2$ | 0 | 4 cycle 10 sec/rev GE $1.4 \times 10^{-5}$ |

## 3.4 GAGE STATIC CALIBRATION

The CRL gage was removed from the aerodynamic molecular beam test cell and installed in the calibration chamber. All the time it was at atmospheric pressure it was sealed in an atmosphere of argon. The calibration tests were conducted with the electronics package providing the same voltages to the gage that it did during the dynamic tests (viz, anode 285v, bias -38v, screen -10v, and emission 0.2v). The calibration procedure consisted of pumping the chamber to its base pressure ($1 \times 10^{-8}$ torr for these tests), then establishing a known flow of the test gas into the system. After the equilibrium pressure was established (i.e., balance between gas flowing in and gas being removed by the chamber pumping system), the chamber pumping system was valved off and the rate of pressure rise in the system was recorded by the CRL gage. Data for various rates of gas additions were recorded. This process was repeated using nitrogen, argon, and oxygen as the test gases.

The gage calibration factors were determined using the following analysis. From the ideal-gas law

$$P_o \frac{dV}{dt} + V\frac{dP_o}{dt} = \frac{dn}{dt} RT$$

For this gas addition system dn/dt RT represents a known gas addition rate and can be represented by dn/dt RT = $P_fK$ where $P_f$ is the forepressure on the gas addition system and can be measured directly with a calibrated bourdon-tube pressure gage and K is the conductance of a previously calibrated leak (see Ref. 4 for leak calibration procedure). Thus the equation of mass balance may be written as

$$P_o \frac{dV}{dt} + V\frac{dP_o}{dt} = P_fK$$

If the pumping system is valved off then

$$P_o \frac{dV}{dt} = 0$$

and

$$V\frac{dP_o}{dt} = P_fK$$

Since the volume of the system can be measured accurately and $P_fK$ is known, then $P_o$ may be replaced by $\alpha I_g$, where $\alpha$ is a calibration factor and $I_g$ is the gage reading, and the equation rearranged to solve for $\alpha$.

$$\alpha = \frac{P_f}{dI_g/dt} \; \frac{K}{V}$$

If several values of $P_f$ are used and a plot of $P_f$ versus dIg/dt made, then the slope of this line may be used to determine a value of $\alpha$. Calibration values were determined for nitrogen, argon, and oxygen.

If during calibration the gas temperature is $T_o$ and the gage temperature is $T_g$, then the actual pressure in the gage $P_g$ is related to the chamber pressure by

$$\frac{P_g}{\sqrt{T_g}} = \frac{P_o}{\sqrt{T_o}}$$

Since the chamber pressure is related to the gage output by the calibration factor $\alpha$, then the pressure in the gage itself is related to its reading by

$$P_g = \alpha Ig\sqrt{\frac{T_g}{T_o}}$$

If this gage is now located in such an environment that its temperature changes to $T_g{}^1$, then its new pressure will be

$$P_g{}^1 = P_g\sqrt{\frac{T_g{}^1}{T_g}}$$

or

$$P_g{}^1 = \alpha Ig\sqrt{\frac{T_g{}^1}{T_g}}$$

When the gage is located in the flow field the number of molecules entering the gage is

$$\dot{n}_{in} = \rho v A k^1$$

where

$\rho$ = molecular density

v = relative gage velocity

A = area of gage orifice

$k^1$ = conductance of tubulation for directed flow

If all the gas accommodates to the gage temperature it will become randomized and the number of gas molecules exiting can be determined from a rate-of-strike calculation.

$$\dot{n}_{out} = \frac{3.513 \times 10^{22} P_g{}^1 A k}{\sqrt{M T_g{}^1}}$$

where

$P_g{}^1$ = gage pressure (in torr)

$T_g{}^1$ = gage temperature

M = molecular weight of gas

k = conductance of tubulation for random flow

Thus for equilibrium conditions since

$$\dot{n}_{in} = \dot{n}_{out}$$

then

$$\rho v A k^1 = \frac{3.513 \times 10^{22} P_g{}^1 A k}{\sqrt{M T_g{}^1}}$$

The pressure in the gage can be related to the gage output by the previously developed calibration relationship and

$$\rho v = \frac{3.513 \times 10^{22} \alpha I_g}{\sqrt{M T_o}} \frac{k}{k^1}$$

It should be noted that in calculating the molecular flux the calibration temperature rather than the actual flight gage temperature should be used. The values of $k^1$ are a function of the velocity of the probe as well as the geometry of the gage tubulation whereas the value of k is only a function of the geometry of the tubulation. For large values of D/ℓ where the gage entrance approximates an orifice, then $k^1 = k = 1$. An estimate of the value of $k/k^1$ for the satellite conditions may be taken from the Hughes report (Ref. 1). These calculations estimate $k/k^1 \approx 0.5$.

# SECTION IV
# RESULTS

Data from the tests in Section 3.2 are shown in Fig. 9. As noted previously, these data were recorded from a GE glass envelope miniature ionization gage, which was installed in the movement mechanism during the checkout portion of the tests.

The CRL gage data were reduced to pressure readings by using the appropriate calibration curves and then plotted with pressure as a function of angle. These curves are reproduced in Fig. 10. Since data reported in Figs. 10b through ℓ were taken with a constant molecular beam flux, then by normalizing to the maximum reading (0-deg azimuth and 4-deg attitude, Fig. 10b) a matrix can be formed where each element is defined as the fraction of maximum signal intensity. This matrix is shown in Fig. 11.

## 4.1 DISCUSSION

The following conclusions are drawn from observations of the operation of the test gage and the data obtained as well as a limited analysis of some of the flight data from the OV1-15 satellite.

### 4.1.1 Calibration

First it should be noted that during these tests the sensitivity of the CRL gage was down by over two orders of magnitude. It is felt that this was caused by the lower voltages supplied by the electronics package. Since the shape of the low sensitivity calibration curve is similar to the curve supplied by the gage manufacturer and is displaced parallel to it on a log-log plot, then the resulting pressure profile data from these tests should be comparable to flight data. These sensitivity calibrations, however, should not be used with satellite data.

### 4.1.2 Sorption

One concern in interpreting the satellite pressure profiles was the possibility of sorption by the gage. If there was appreciable sorption this would result in a saturation when the gage was facing forward and at its highest pressure level, and then a desorption as the gage rotated to face rearward. This desorbing gas would thus act as a gas source and add to the gas pressure and distort the "true" pressure reading. When the gage was rotating from a rearward to a forward position the sorbing surfaces would act as a pump, thus lowering the gage pressure. For a gage having appreciable sorption the total effect during each revolution would be to skew the pressure profile. The satellite data and the test data both show asymmetrical profiles. However, it is not felt that sorption is the cause of this asymmetry for the following reasons:

1. The pressure profiles taken by the glass envelope gage and the titanium-ceramic CRL gage are the same, and there is no experimental evidence to suspect appreciable sorption of nitrogen by Pyrex® glass.

2. The static profile and the dynamic profiles taken with the CRL gage are identical, and sufficient time was allowed during the static cycle for the gage to equilibrate at each point.

3. The dynamic tests consisted of rotating the gage both clockwise and counterclockwise. These data are identical, indicating that for any specific angle each data point is the same, regardless of whether the gage approached it from a high or a low pressure reading.

The more obvious cause for asymmetry is found in the gage orifice. Two results would indicate this as the main cause:

1. The orifice is asymmetric about the azimuthal plane, and data for constant azimuth and varying attitude are also asymmetric.

2. The gage orifice is symmetric about the attitude plane, and data for changing azimuth angle and constant attitude are also symmetric.

#### 4.1.3 Aspect Angle Correction Factor

Because the azimuth and attitude profiles are not identical, then any angle of attack must be defined by the appropriate azimuth and attitude angles before the proper angle correction factor can be chosen from the matrix presented as Fig. 11. Unfortunately, there is no unique combination of azimuth and attitude angle for any particular aspect angle (or angle of attack) of the gage. The importance of this fact can be noted by comparing Figs. 12, 13, and 14. Figure 12 is a profile recorded in the azimuthal plane ($\alpha$ = constant) and attitude varying ($\beta = \pm 60$ deg). Figure 13 is a profile recorded in the attitude plane ($\beta$ = constant), and azimuth varying ($\alpha = \pm 60$ deg). Figure 14 is a measured profile where the aspect angle $\gamma$ varies and is defined as

$$\cos \gamma = \cos \alpha \cos \beta$$

All three of these profiles sweep through the same range of aspect angles and are taken with the same beam flux, yet it is quite evident that they describe quite different pressure profiles.

#### 4.1.4 Theoretically Predicted Aspect Angle Correction Factor

A theoretical study of probes operating in the free-molecular regime was conducted at the University of Toronto by Hughes (Ref. 1). From this study a plot of the expected gage readings for a tubulated ion gage rotating in a molecular flow field can be provided. The dimensions of the CRL gage orifice are shown in Fig. 15. From these dimensions a value of D (diameter-to-length ratio) is calculated. Since the geometry is not a simple tube there must be some reservations attached to the value used for these comparisons.

Figure 16a is a plot of predicted gage reading (normalized to $2.9 \times 10^{-5}$ torr) using values of S = 10, D = 0.75, and $\alpha$ varying from -90 to 90 deg. Figures 16b and c illustrate the predicted narrowing of the pressure profile as various tubulations (D ratios) are considered.

A comparison of Figs. 12 and 16a indicates that there is fairly good agreement between the measured and predicted profile for this orientation of the gage. For this particular comparison the tubulation factor (D = 0.75) ignores the effects of the negative ion deflection plates and only considers the circular tubulation of the gage. By appropriate choices of this tubulation factor, the theoretically predicted pressures can be matched to other measured profiles (compare Figs. 14 and 16b). However, there seems to be little profit in this exercise since there are no logical rules to convert the complex entrance geometry of the actual gage into an equivalent tube diameter-to-length ratio.

#### 4.1.5 General Comments

There are several general observations which may be made after examining some of the semireduced orbital data and comparing it to the ground test data.

1. The satellite pressure profile for the limited data examined, where the minimum aspect angle approaches zero, is in general narrower than that predicted by the Hughes report. From theoretical considerations errors in the value of the speed ratio attributable to uncertainties in the upper atmospheric temperature should have very little effect on the general shape of the profile (Figs. 16a, d, and e). Specular rather than diffuse reflections on the walls of the gage entrance should broaden rather than narrow the profile. Combinations of azimuth and attitude angles as shown in the ground test data can be chosen to match the flight pressure profiles. However, there is no assurance that these are indeed the actual orientations of the gage during the particular rotations considered.

2. On several occasions during calibration the gage output started to oscillate. No apparent cause could be determined and the parasitic oscillations stopped as unpredictably as they started. Evidence of similar oscillations is apparent in the satellite data (Fig. 17). It is suggested that such oscillations in the satellite data are not necessarily evidence of gage encounters with ion showers or spurious electromagnetic disturbance in the upper atmosphere.

3. Occasionally, the reduced data indicated a failure to switch ranges during a pressure fluctuation. In most cases this was traced to a data reduction problem and a failure of the computer to catch the range shift. However, during rate of pressure rise measurements for calibration purposes it was noted that it is possible for the gage to obviously change scales without indicating a range shift.

4. The several inversions of parts of the pressure profiles recorded on earlier data reductions were all traced to computer problems.

## SECTION V
## CONCLUSIONS

From these studies it may be concluded that the basic approach of the theoretical analysis is sound; however, the complex entrance geometry of this particular gage leads to considerable doubt as to what effective tubulation (D) ratio should be used for a particular aspect angle. The matrix determined from these tests should be applicable to satellite data; however, since the chamber background pressure is becoming a major contributor to gage pressures at angles beyond ±60 deg, it is suggested that these factors be used only within these limits. Because of the asymmetry in the matrix it will be necessary to define both the attitude and azimuth angle for each aspect angle recorded in the satellite data in order to choose the appropriate correction factor.

During these tests there were no indications of sorption or desorption problems with the gage. Spurious oscillations in the gage output were observed, but it was not determined if these were attributable to discharges within the gage or were produced in the electronics package.

## REFERENCES


1. Hughes, P. C. "Theory for the Free Molecule Impact Probe at an Arbitrary Angle of Attack." UTIAS Report No. 103, May 1965.

2. Caldwell, R. L., Busby, M. R., and Brown, R. F. "Spatial Distributions from 285 to 2500°K Argon Beams Scattered from an Undefined Copper Surface at Temperatures between 36 and 285°K." AEDC-TR-69-142 (AD698325), December 1969.

3. Brown, R. F. and Heald, J. H., Jr. "Performance of an Aerodynamic Molecular Beam Chamber for Cryopumping and Adsorption Pumping Studies." Journal of Spacecraft and Rockets, Vol. 4, No. 4, 1967, pp. 476 to 480.

4. Dawbarn, R. "Cryosorption of Hydrogen by 12-20°K Carbon Dioxide Cryodeposits." AEDC-TR-67-125 (AD655067), July 1967.

5. Ruby, E. C., Brown, R. F., and Busby, M. R. "The Effects of Condensation on the Flow Field Properties in Free-Jet Expansions of Argon." AEDC-TR-70-142 (AD710616), August 1970.

6. Piccirilli, J. "Density Gage System - Final Report." AS&E 2173, January 1969.

# APPENDIX
# ILLUSTRATIONS

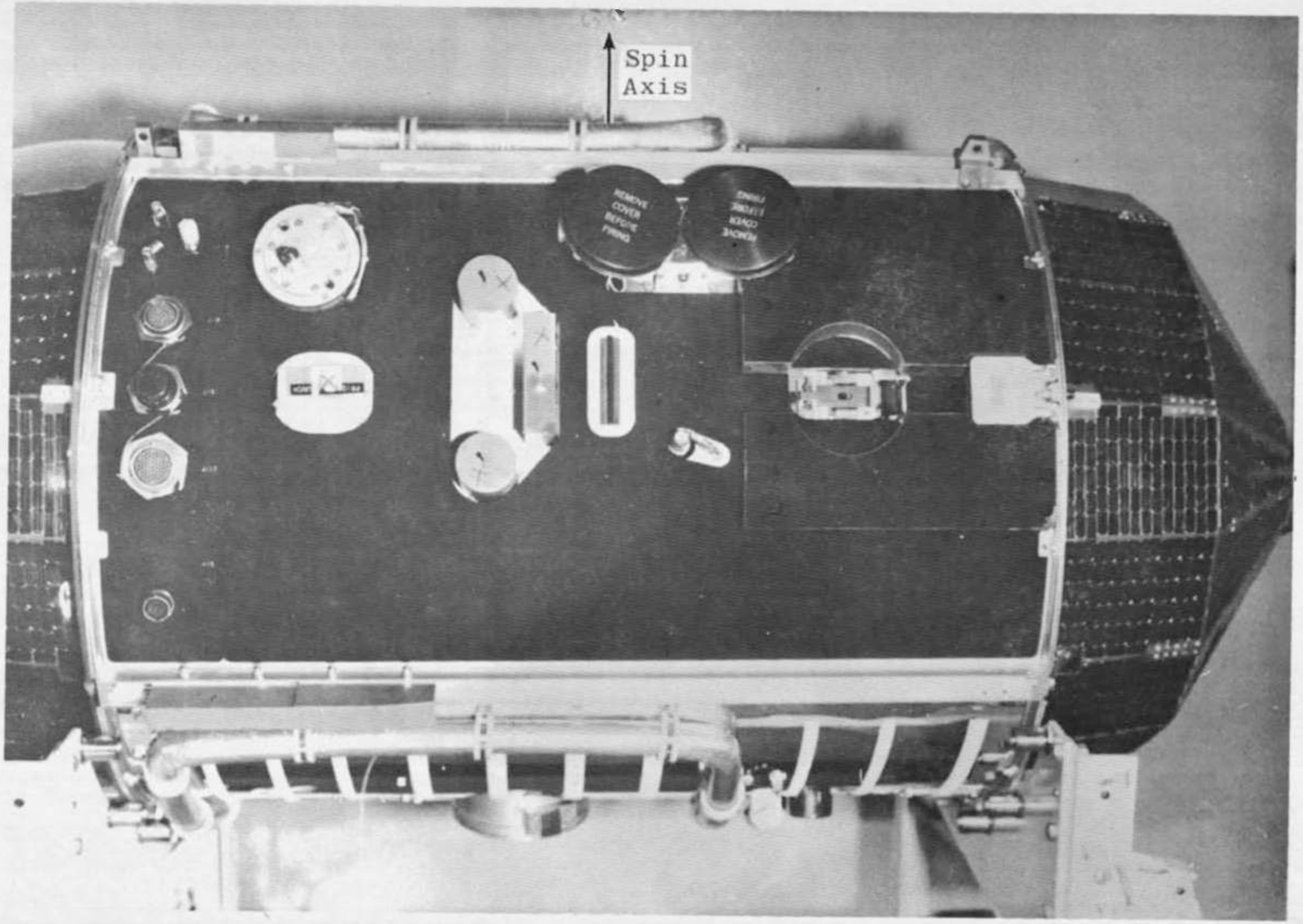


Fig. 1 OV1-15 Satellite

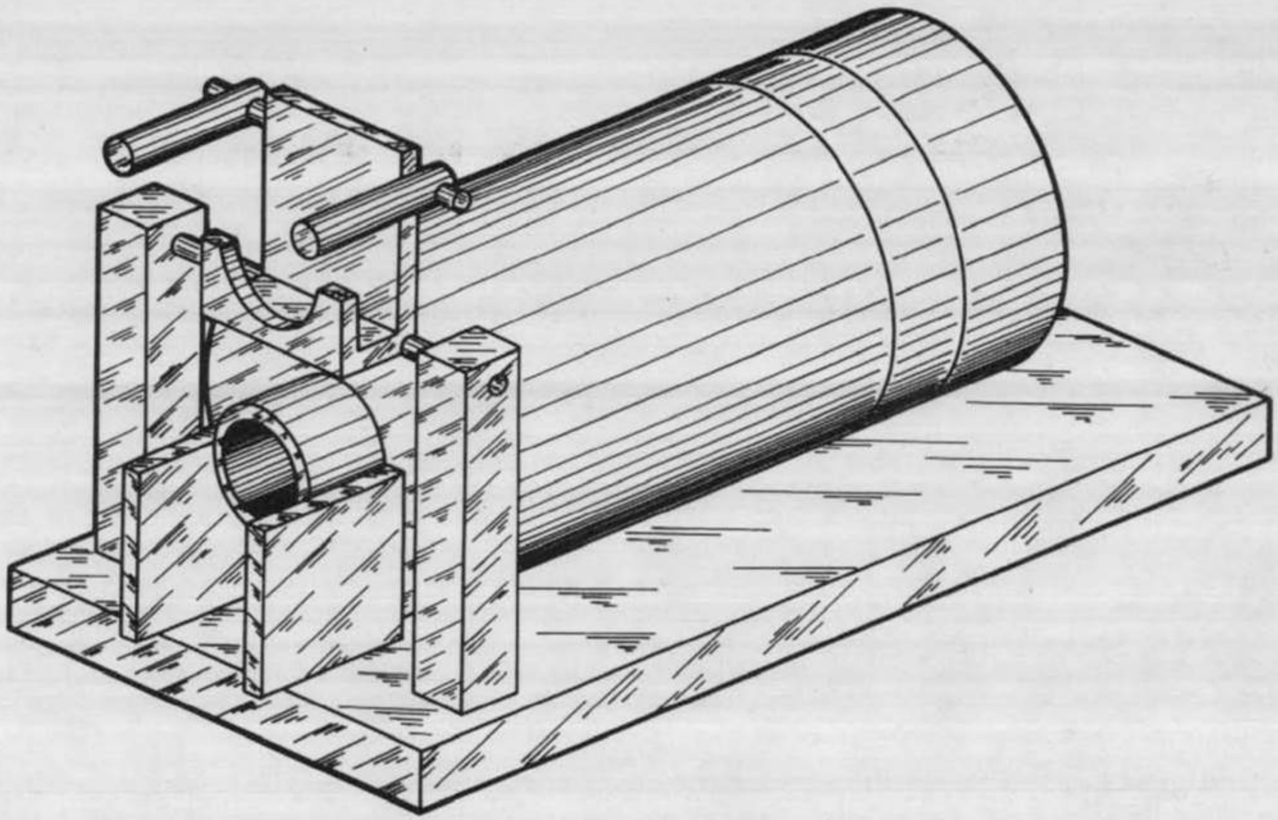

Fig. 2 View of Gage Entrance

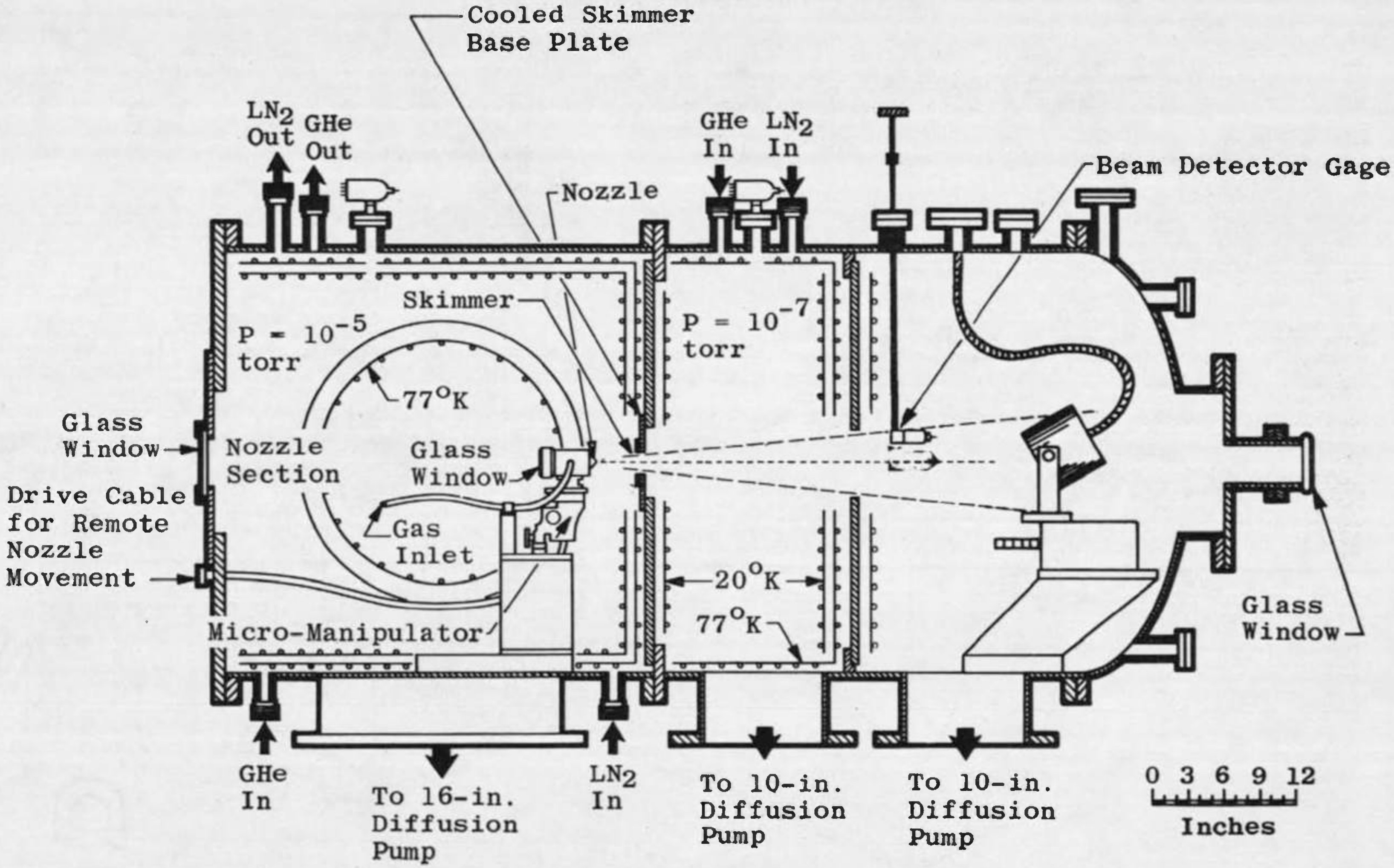


Fig. 3 Schematic of Molecular Beam Chamber

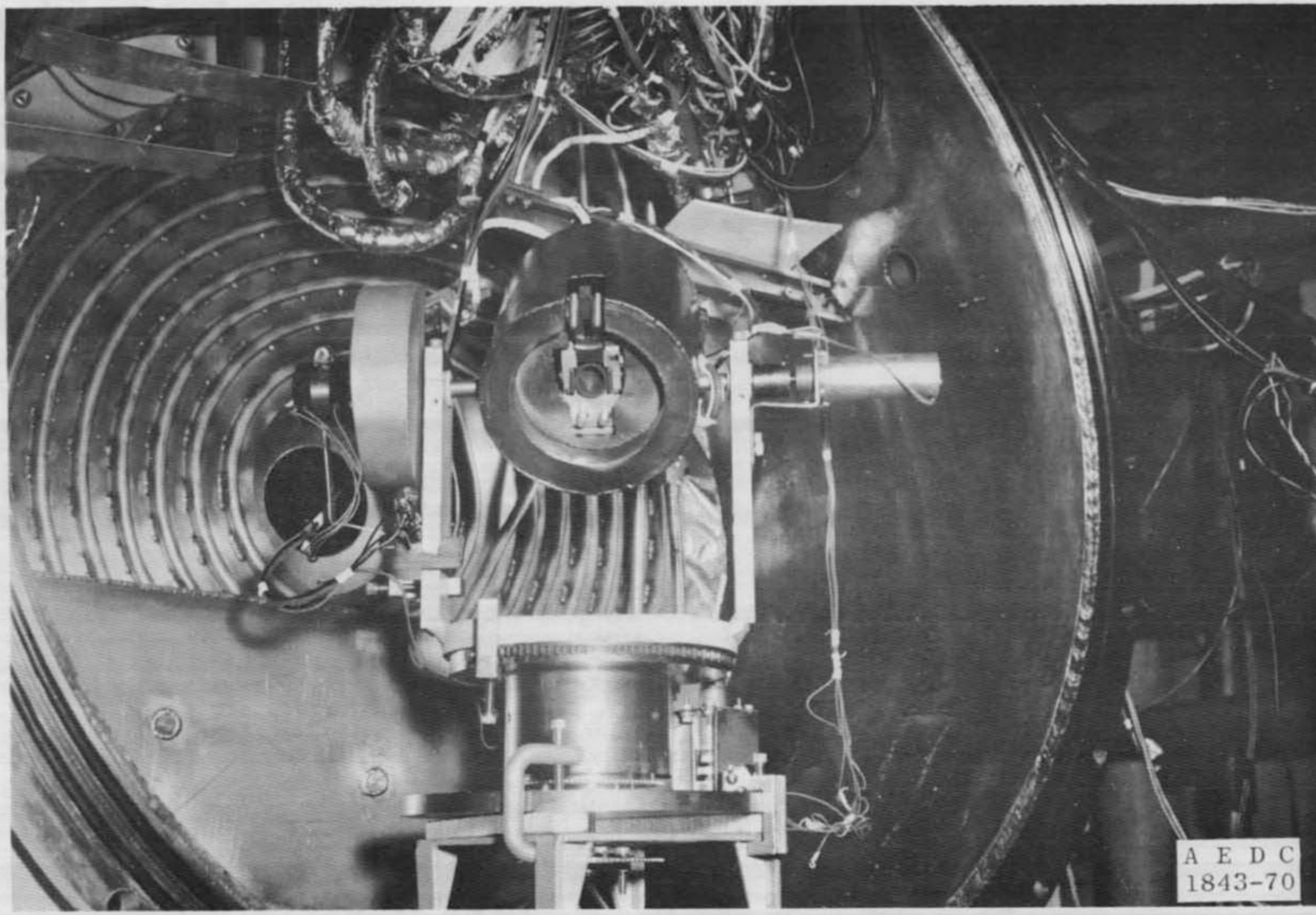


Fig. 4 View of Gage Movement Mechanism

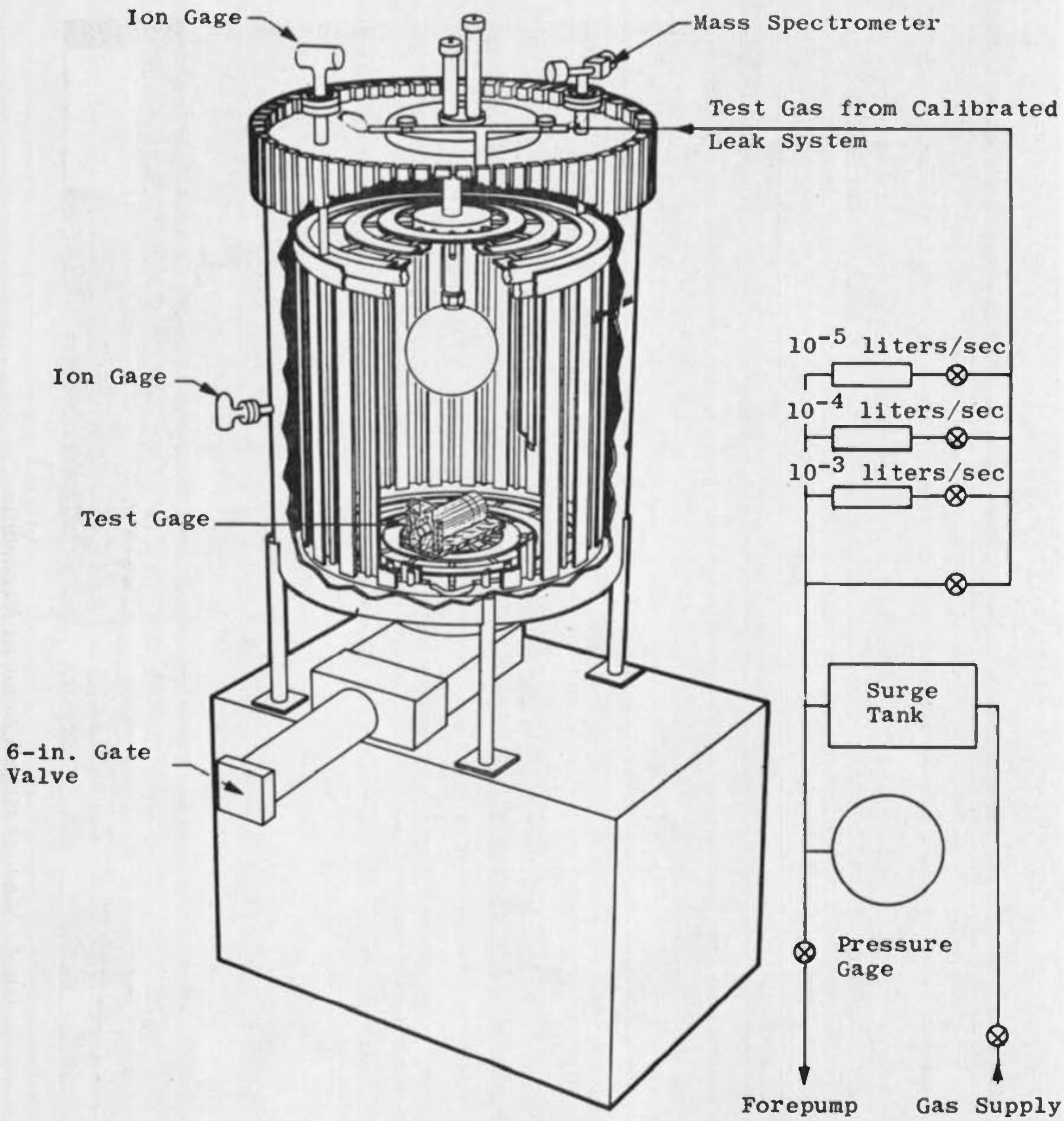


Fig. 5 Schematic of Gage Calibration Chamber

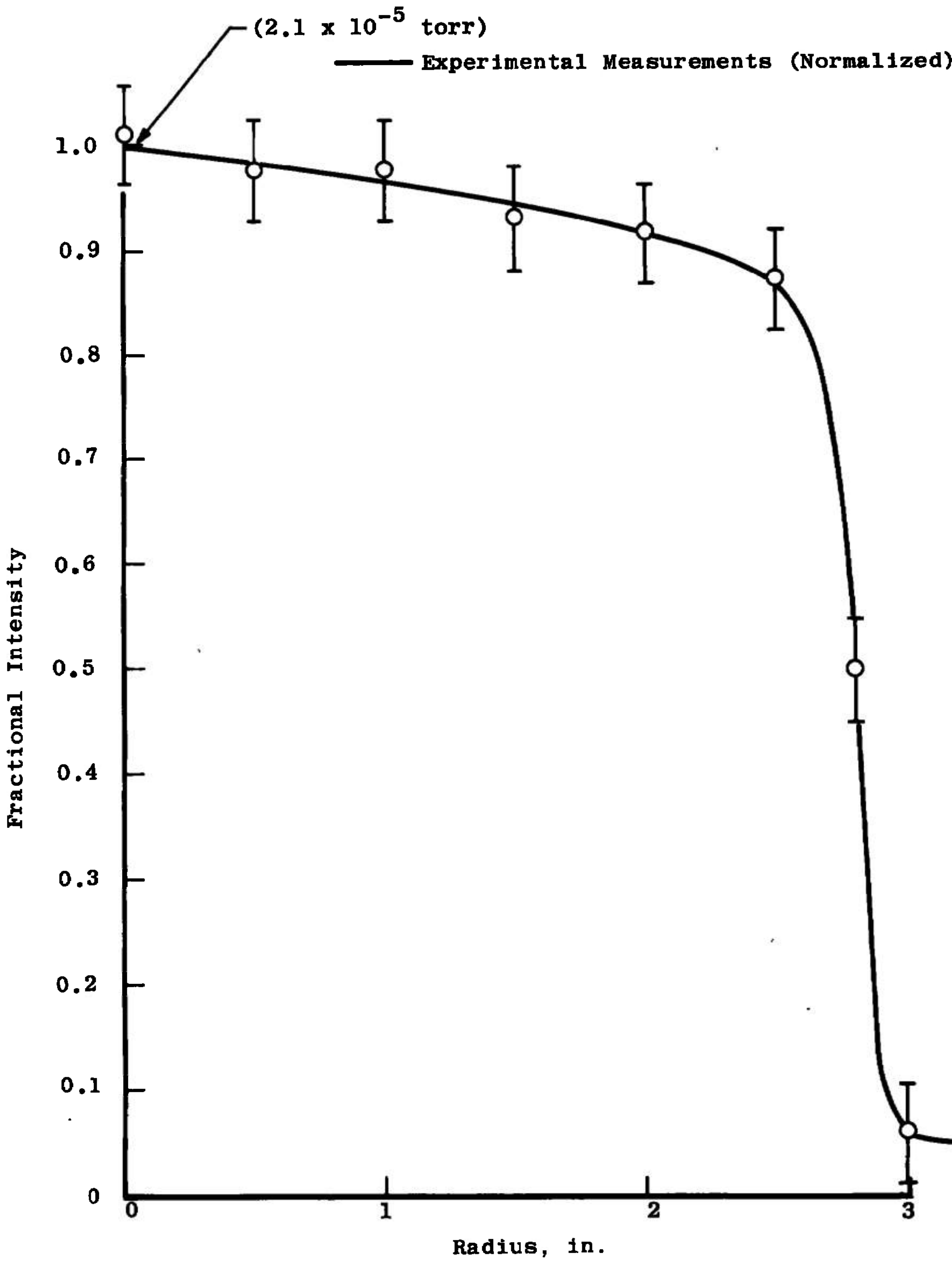


Fig. 6 Molecular Beam Profile

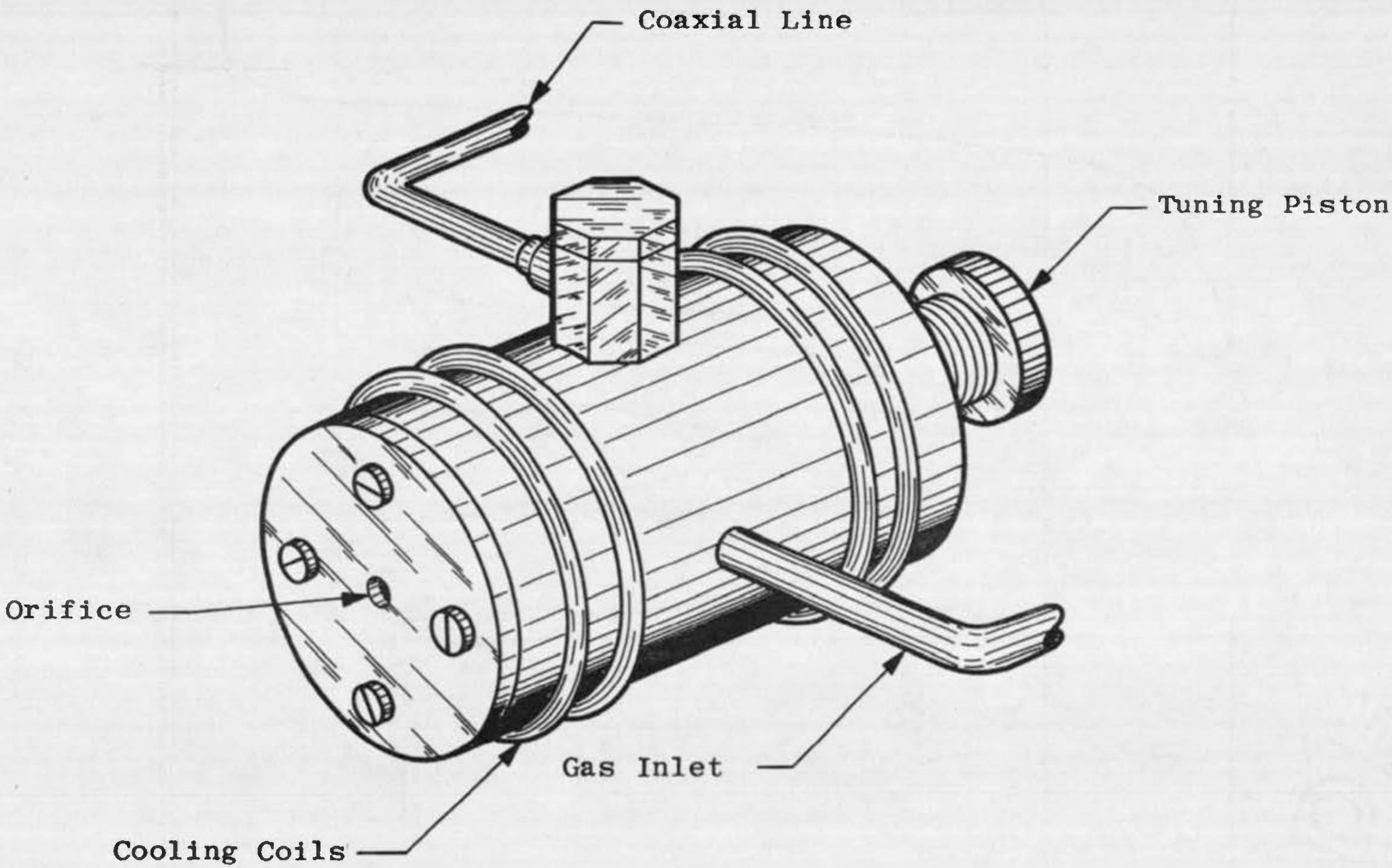


Fig. 7 View of Microwave Cavity

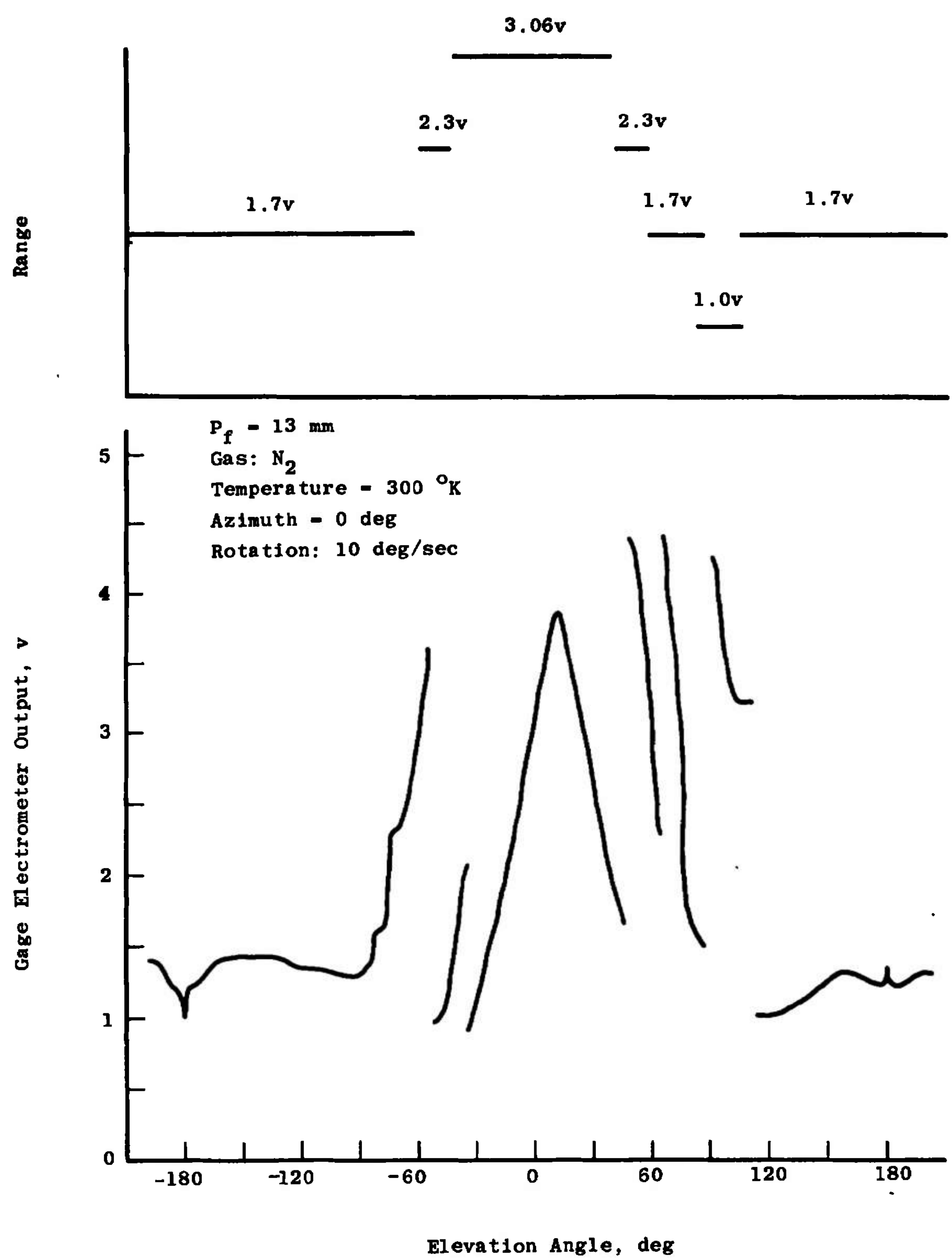


Fig. 8 Sample of Density Signal Output during One Rotation

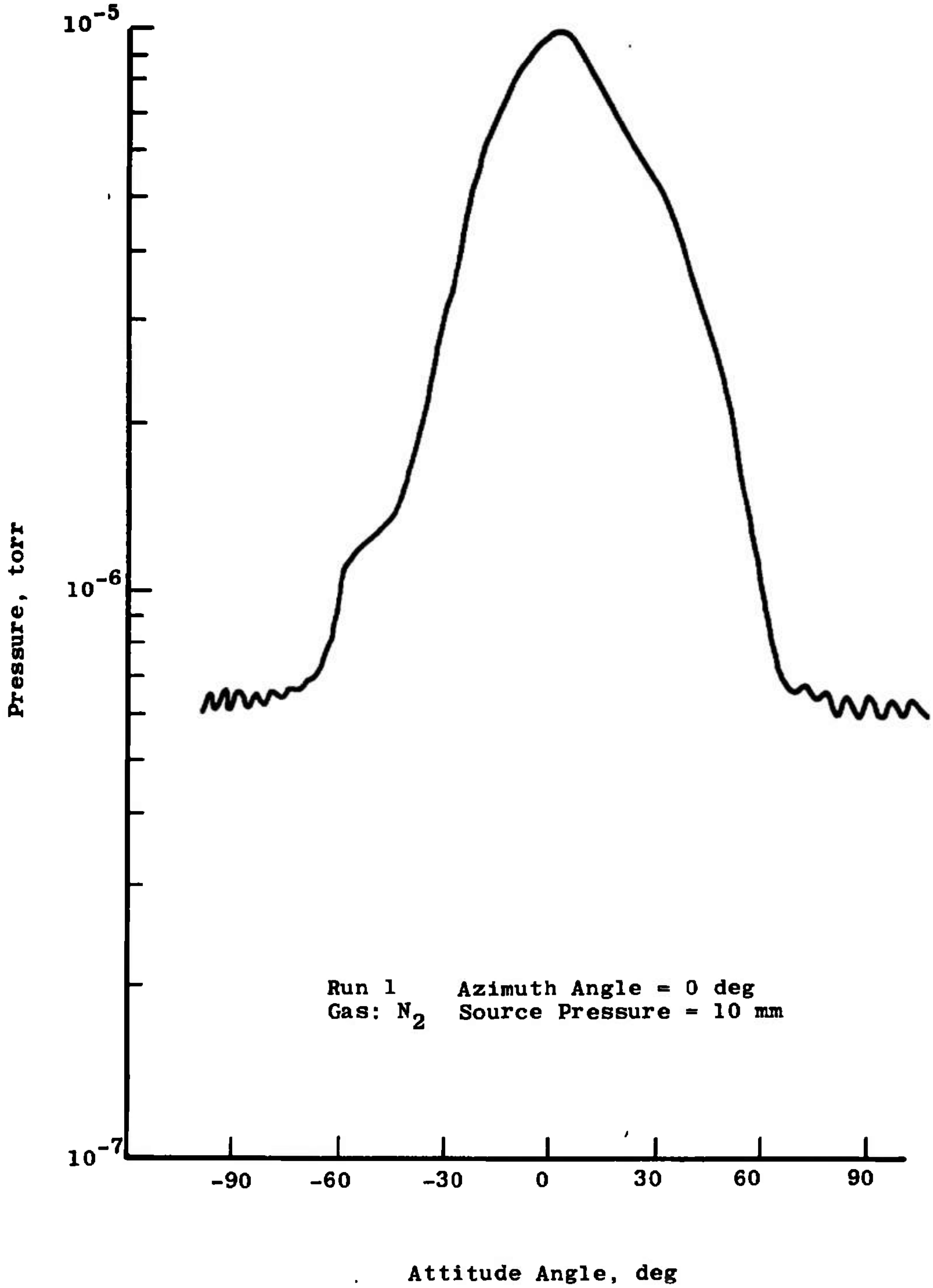


a. Run 1
Fig. 9 Data from GE Gage

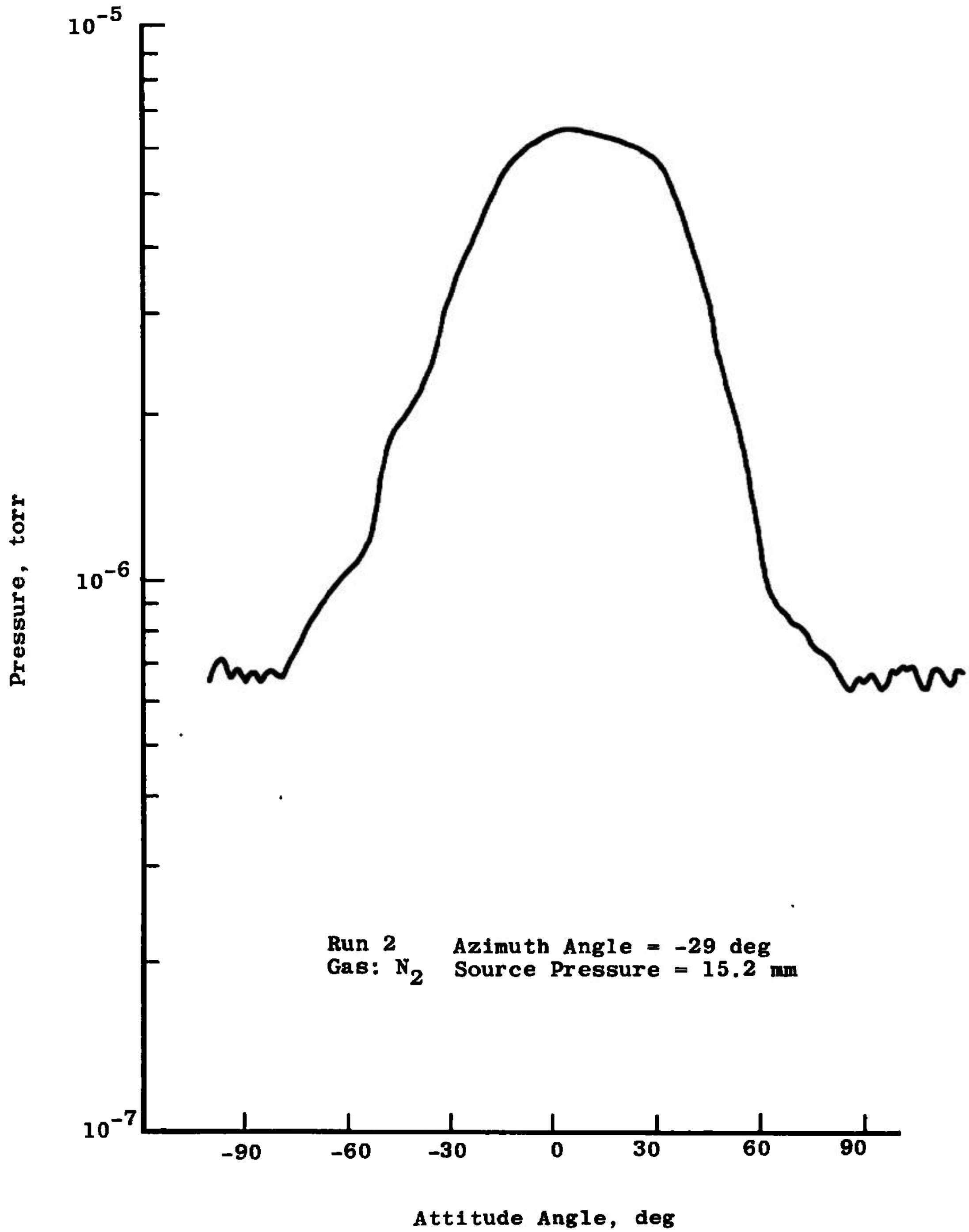


b. Run 2
Fig. 9 Continued

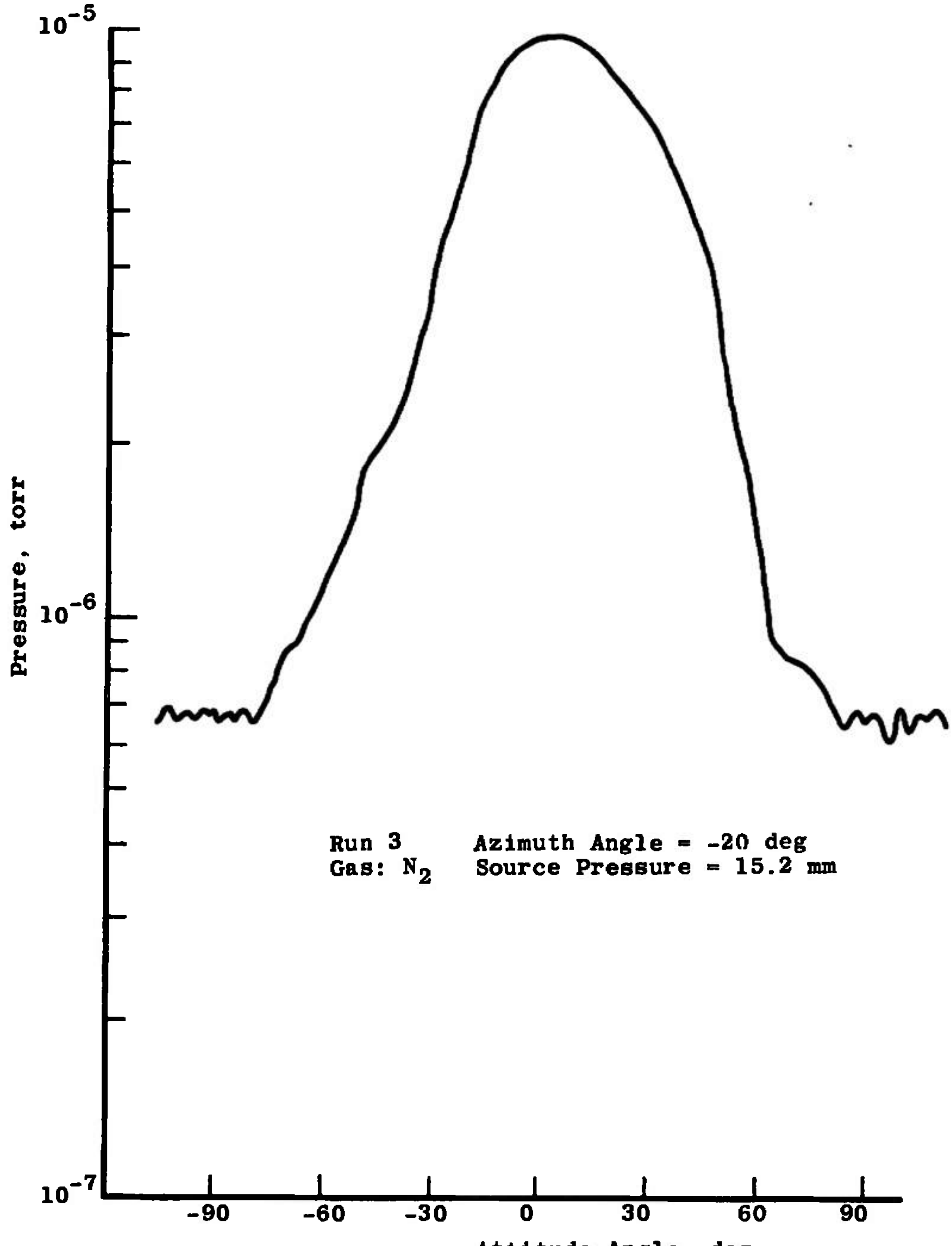


c. Run 3
Fig. 9 Continued

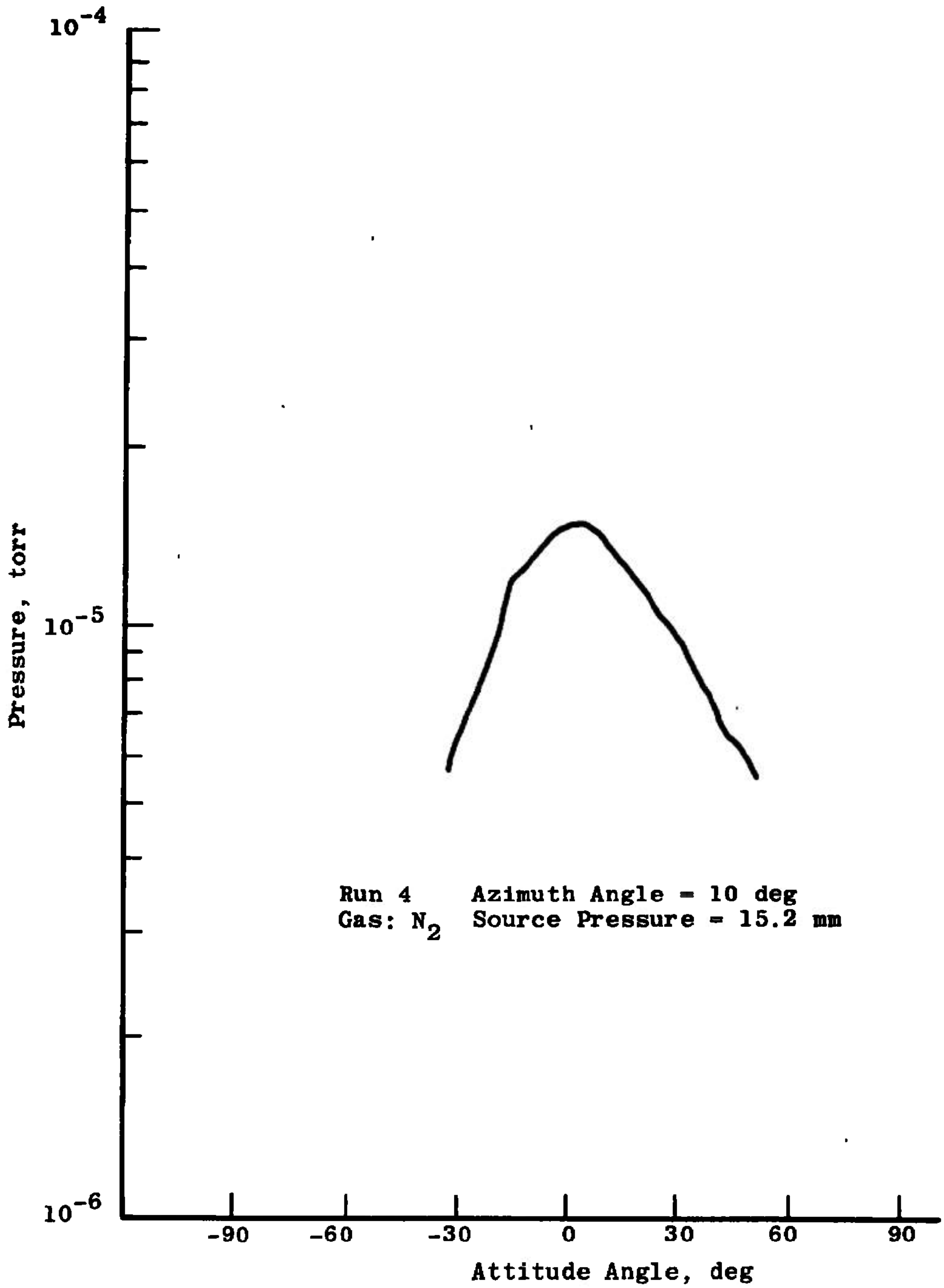


d. Run 4
Fig. 9 Continued

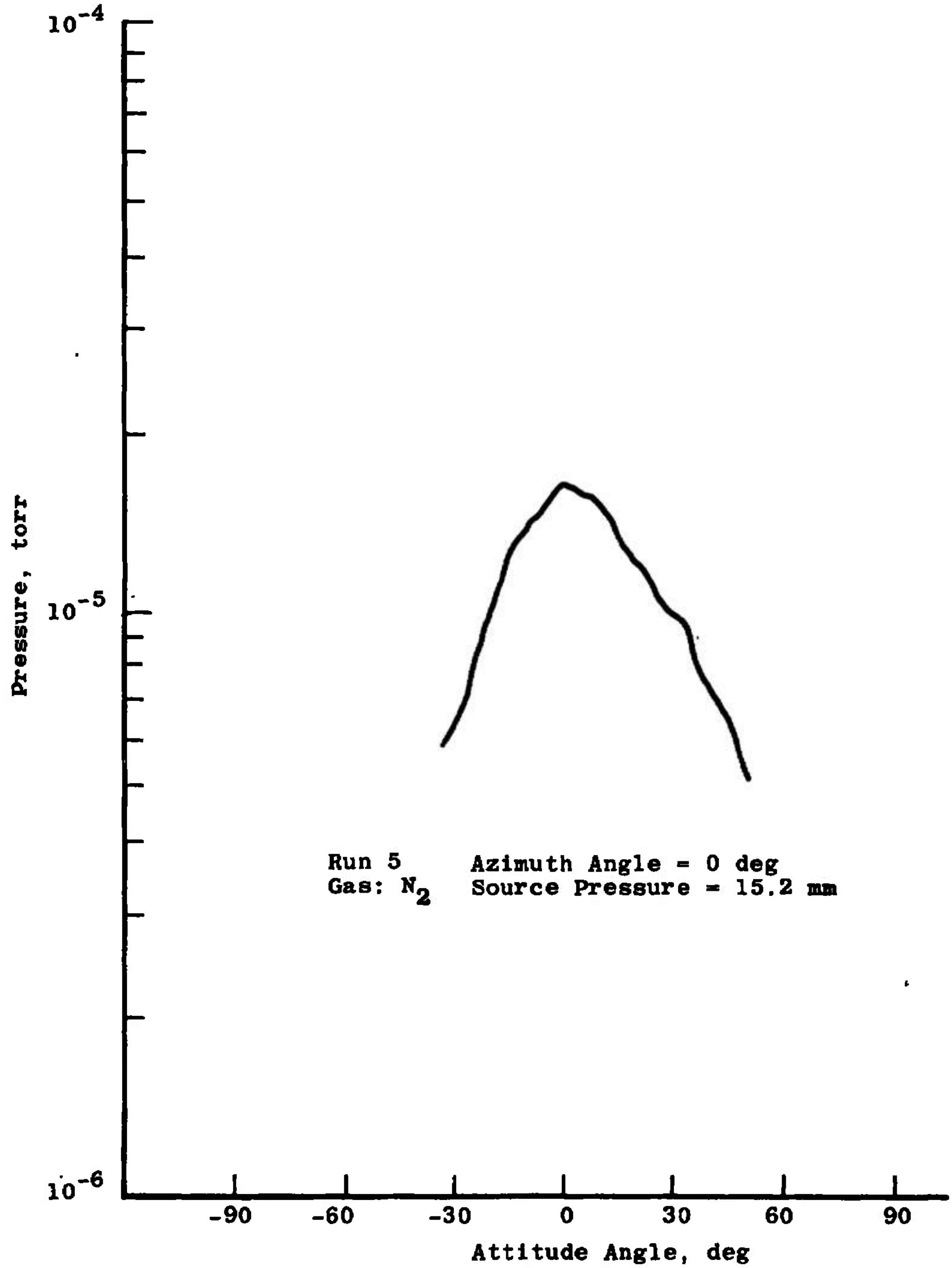


e. Run 5
Fig. 9 Continued

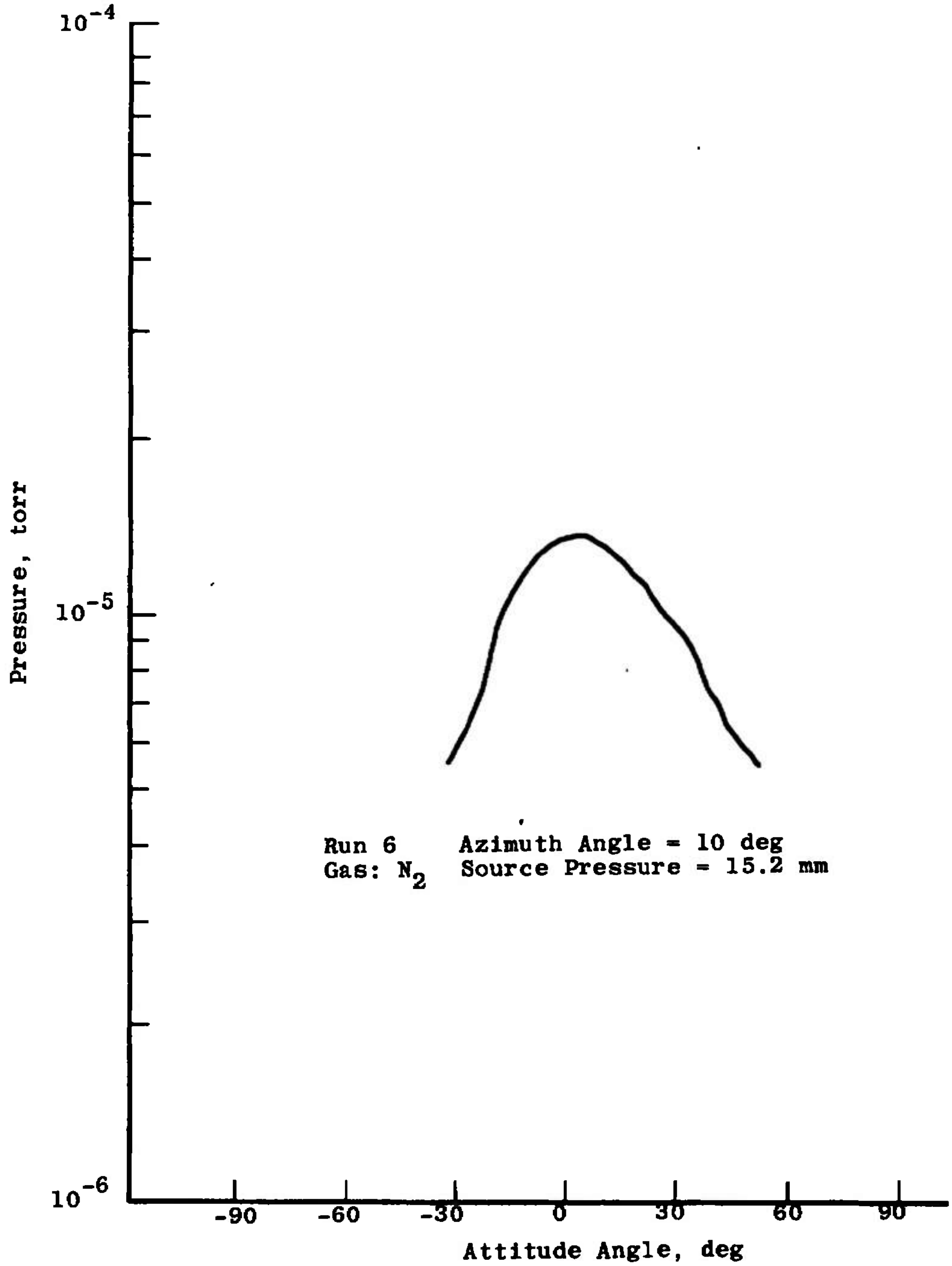


f. Run 6
Fig. 9 Continued

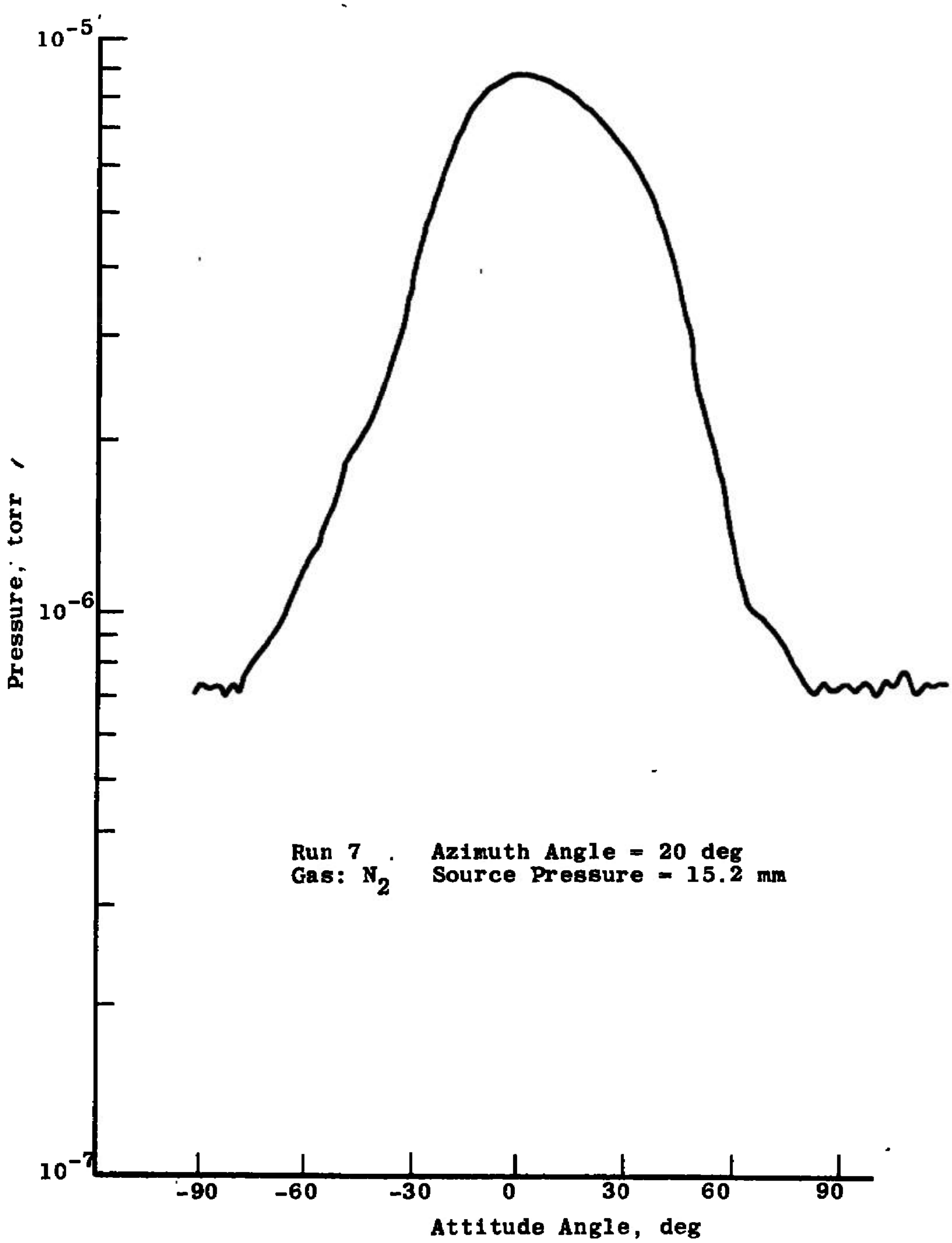


g. Run 7
Fig. 9 Continued

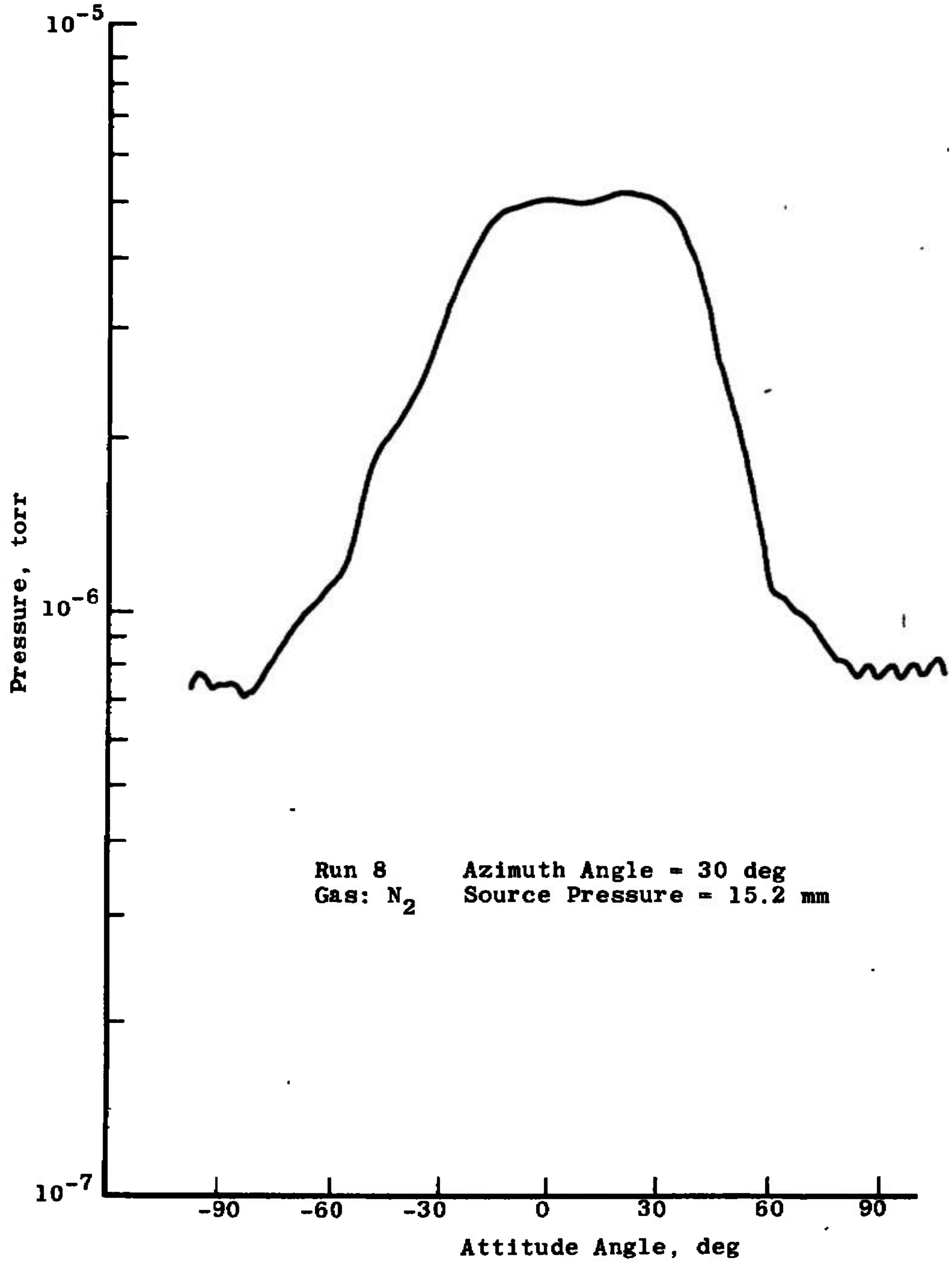


h. Run 8
Fig. 9 Continued

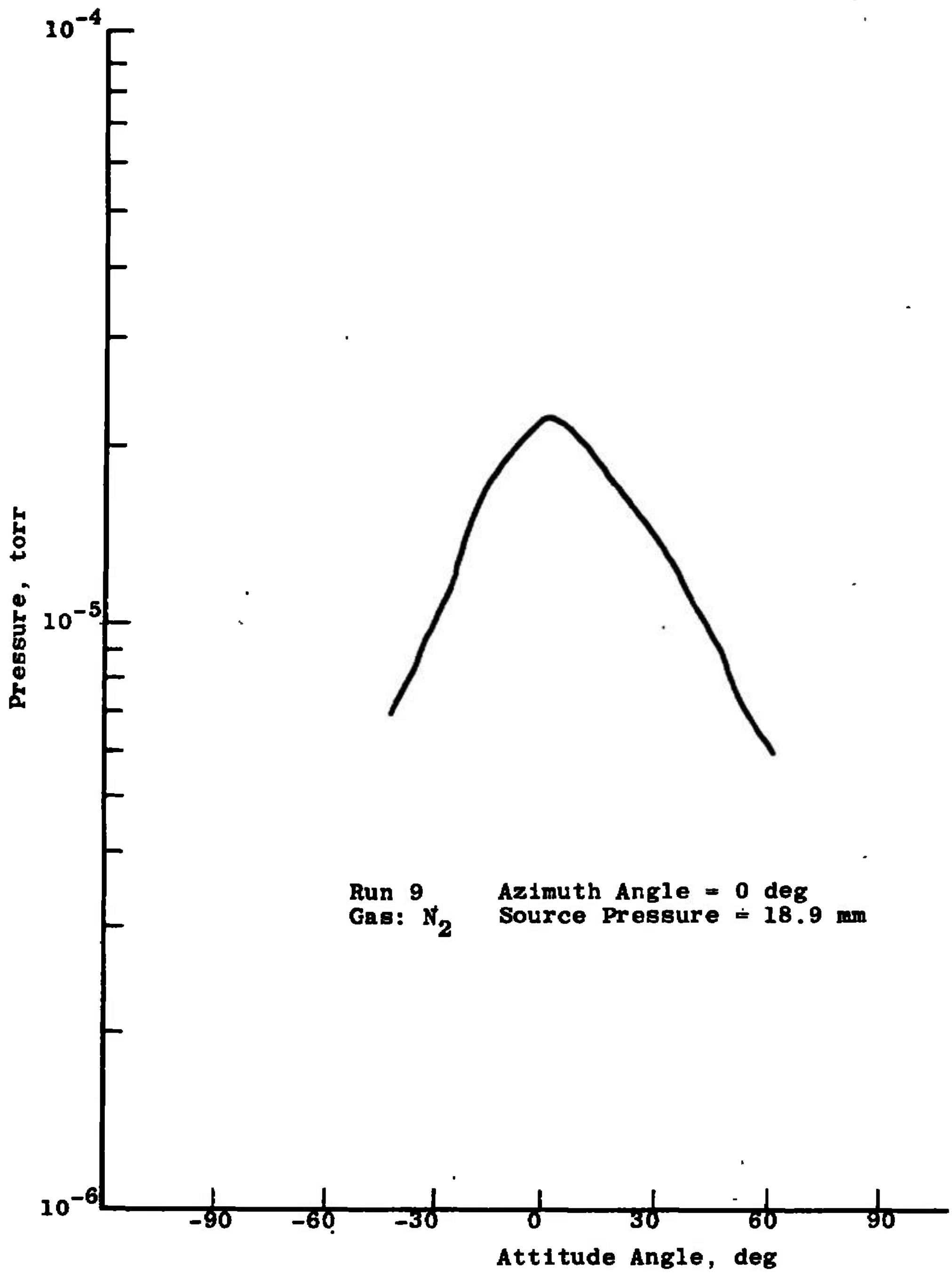


i. Run 9
Fig. 9 Continued

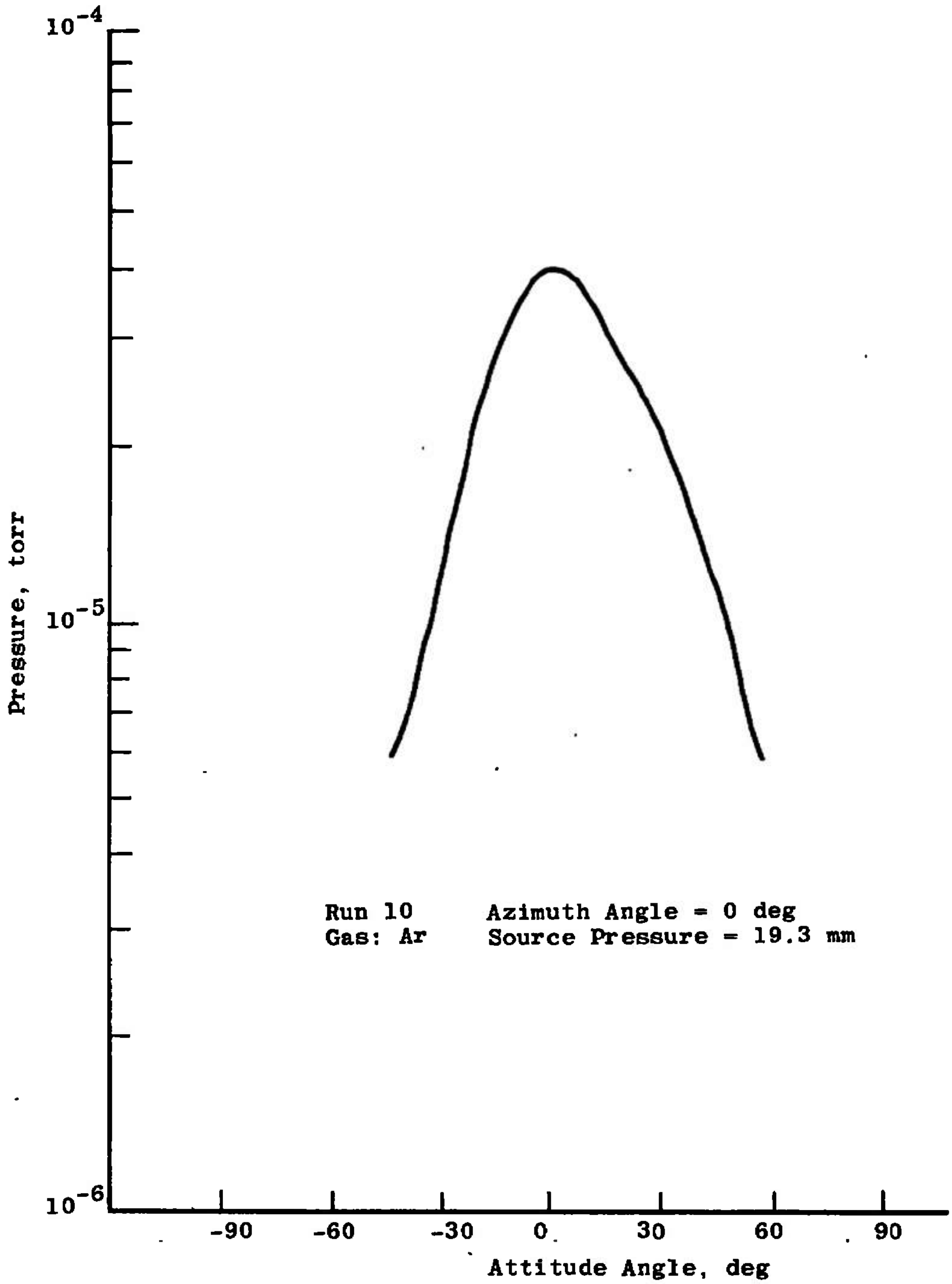


j. Run 10
Fig. 9 Continued

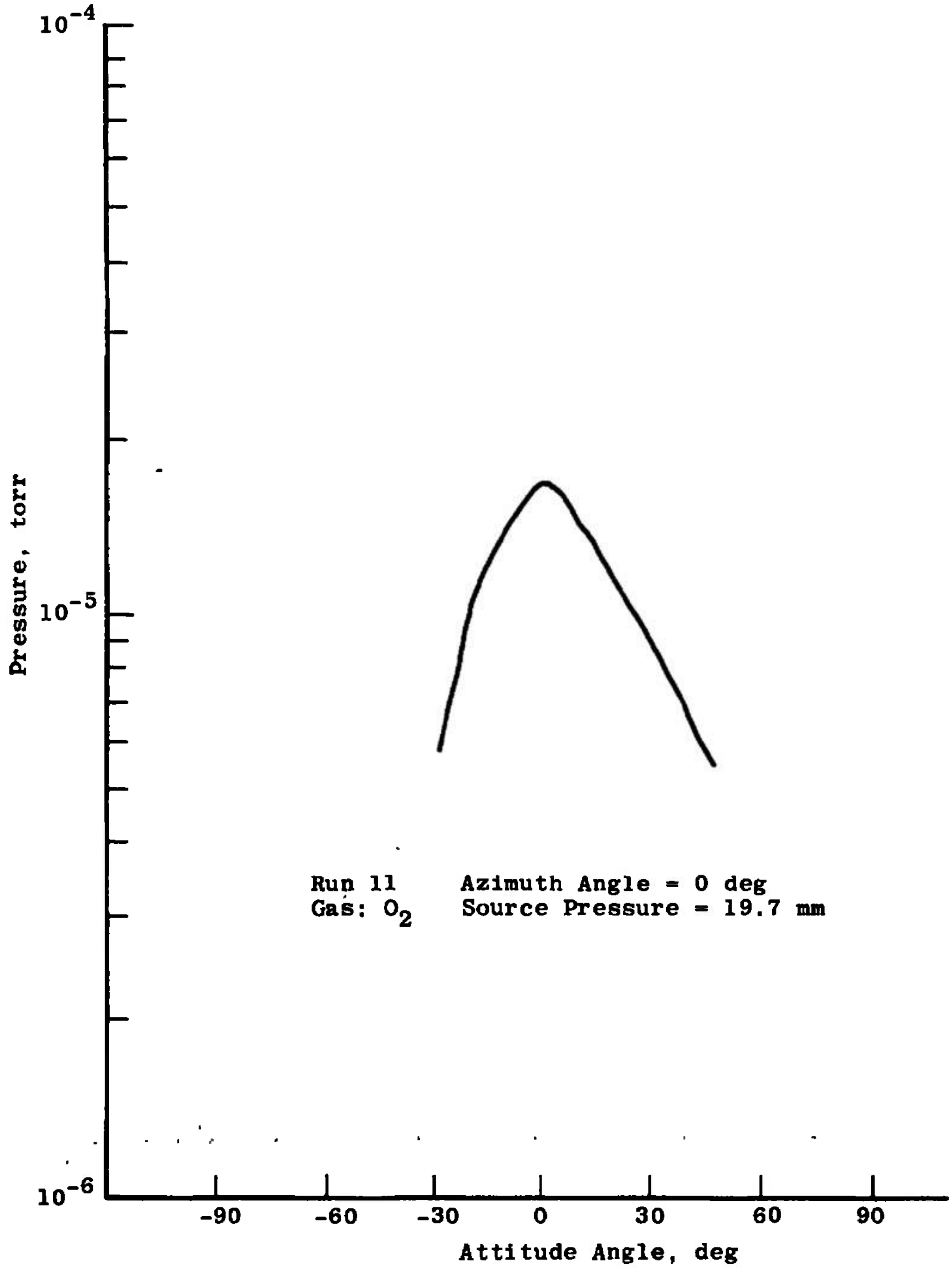


k. Run 11
Fig. 9 Continued

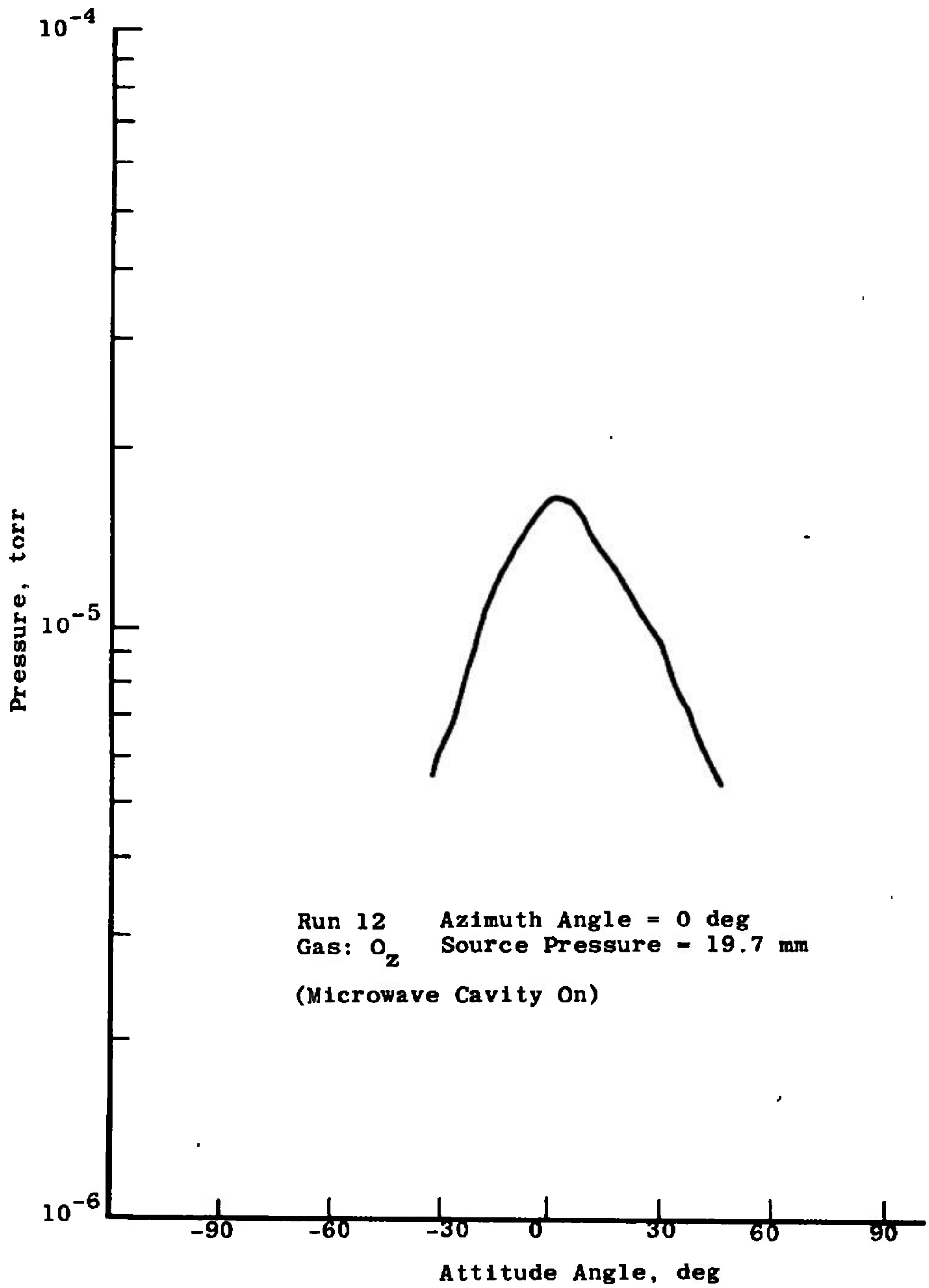


l. Run 12
Fig. 9 Continued

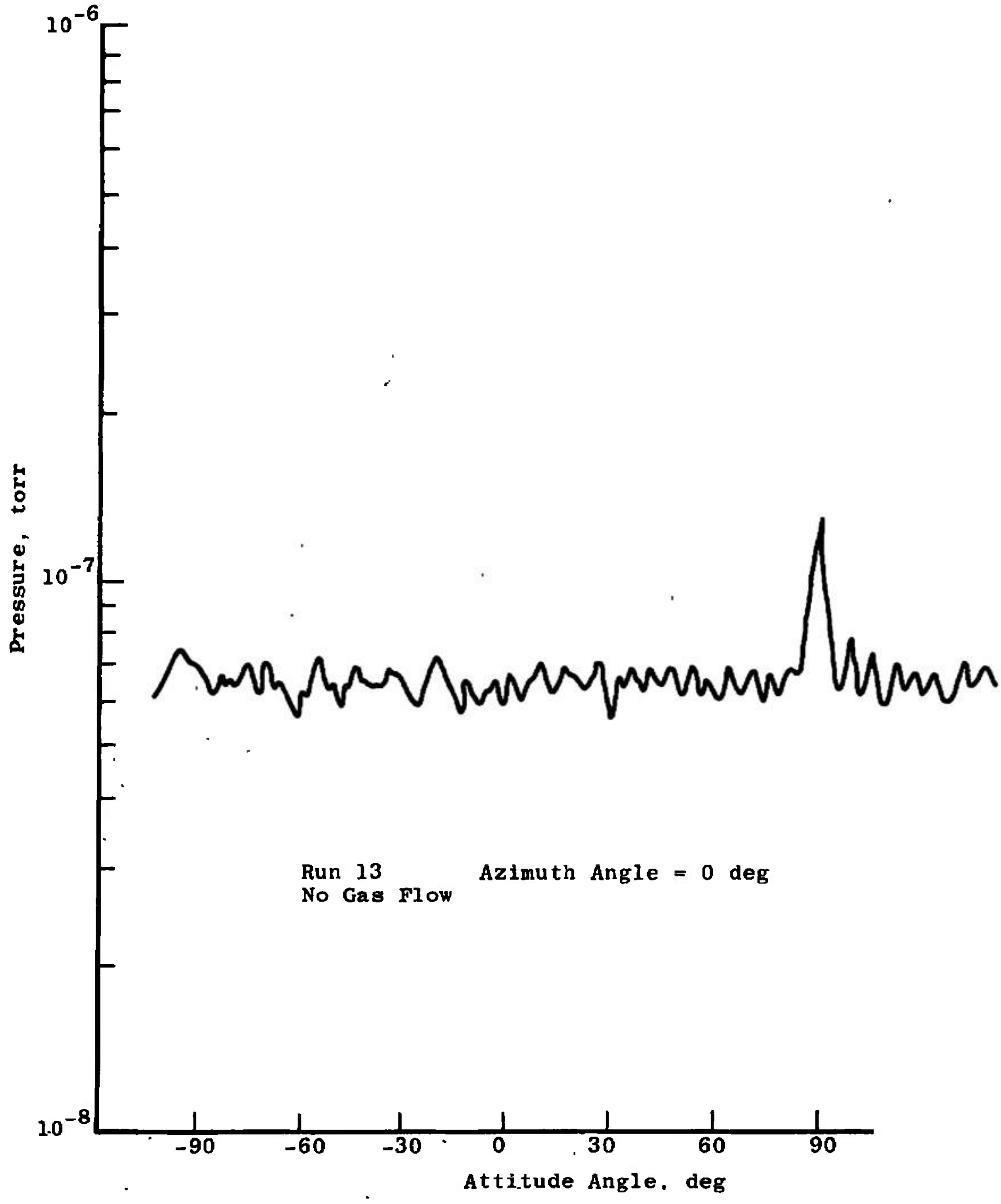


m. Run 13
Fig. 9 Concluded

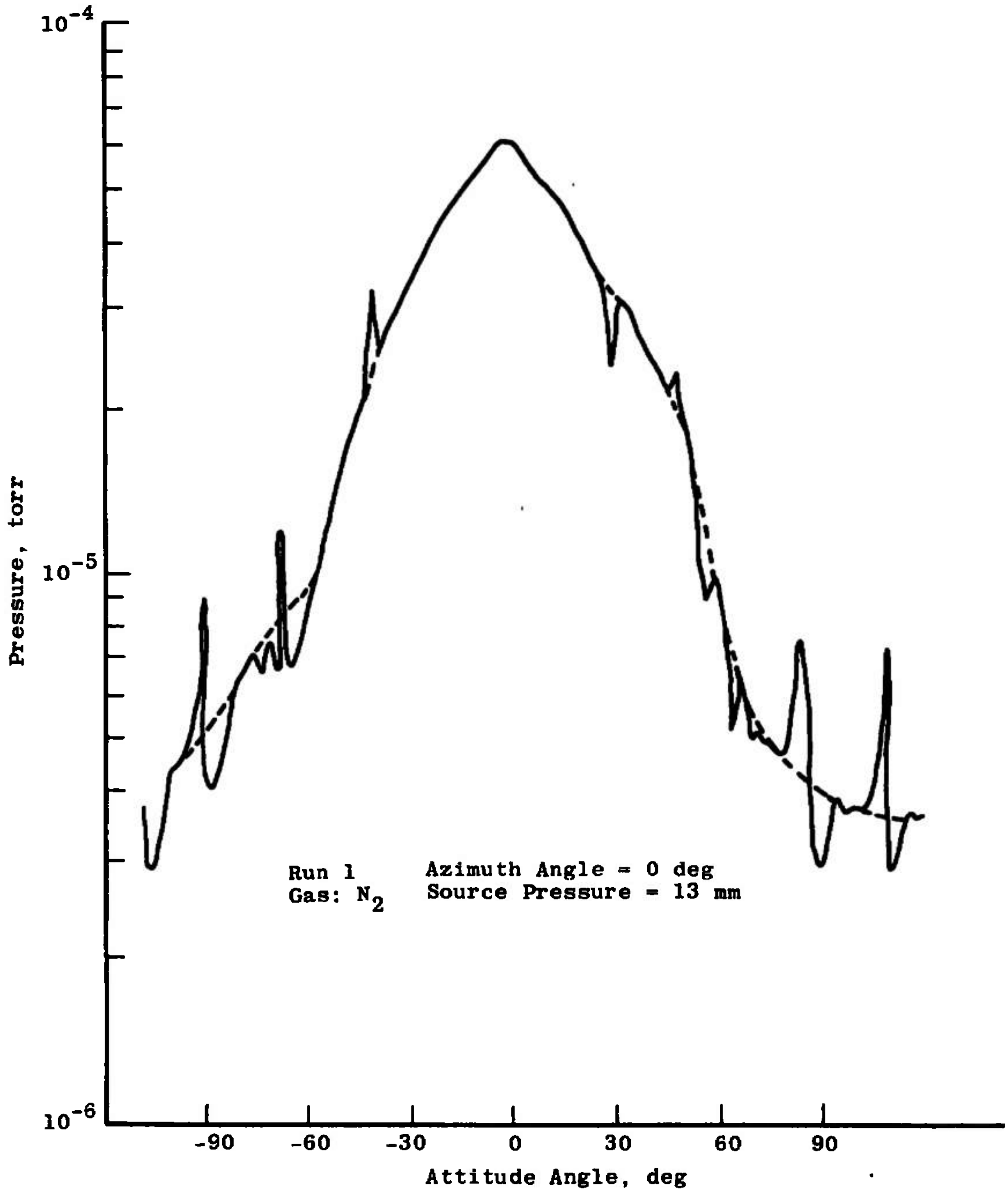


a. Run 1
Fig. 10 Data from CRL Gage

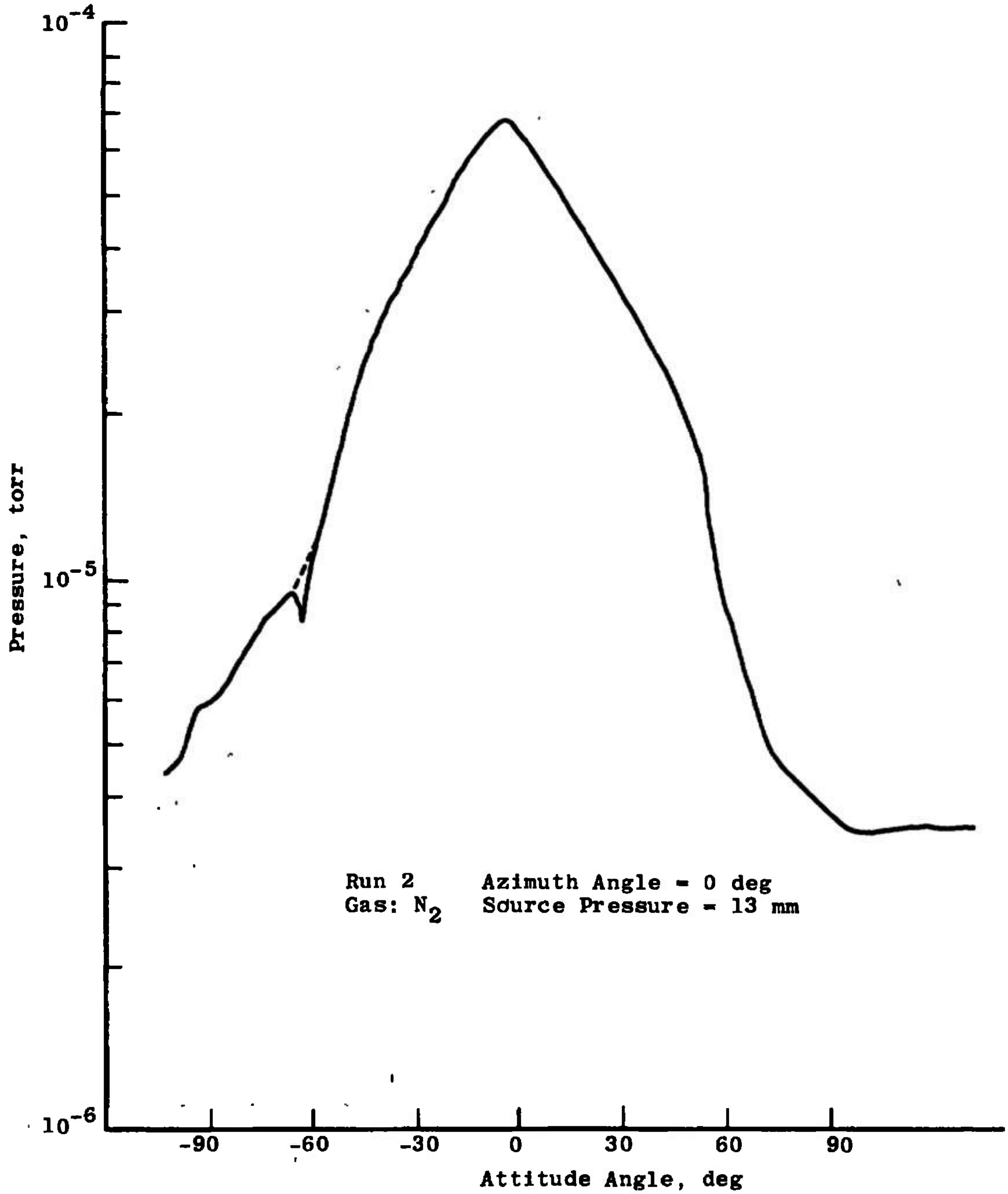


b. Run 2
Fig. 10 Continued

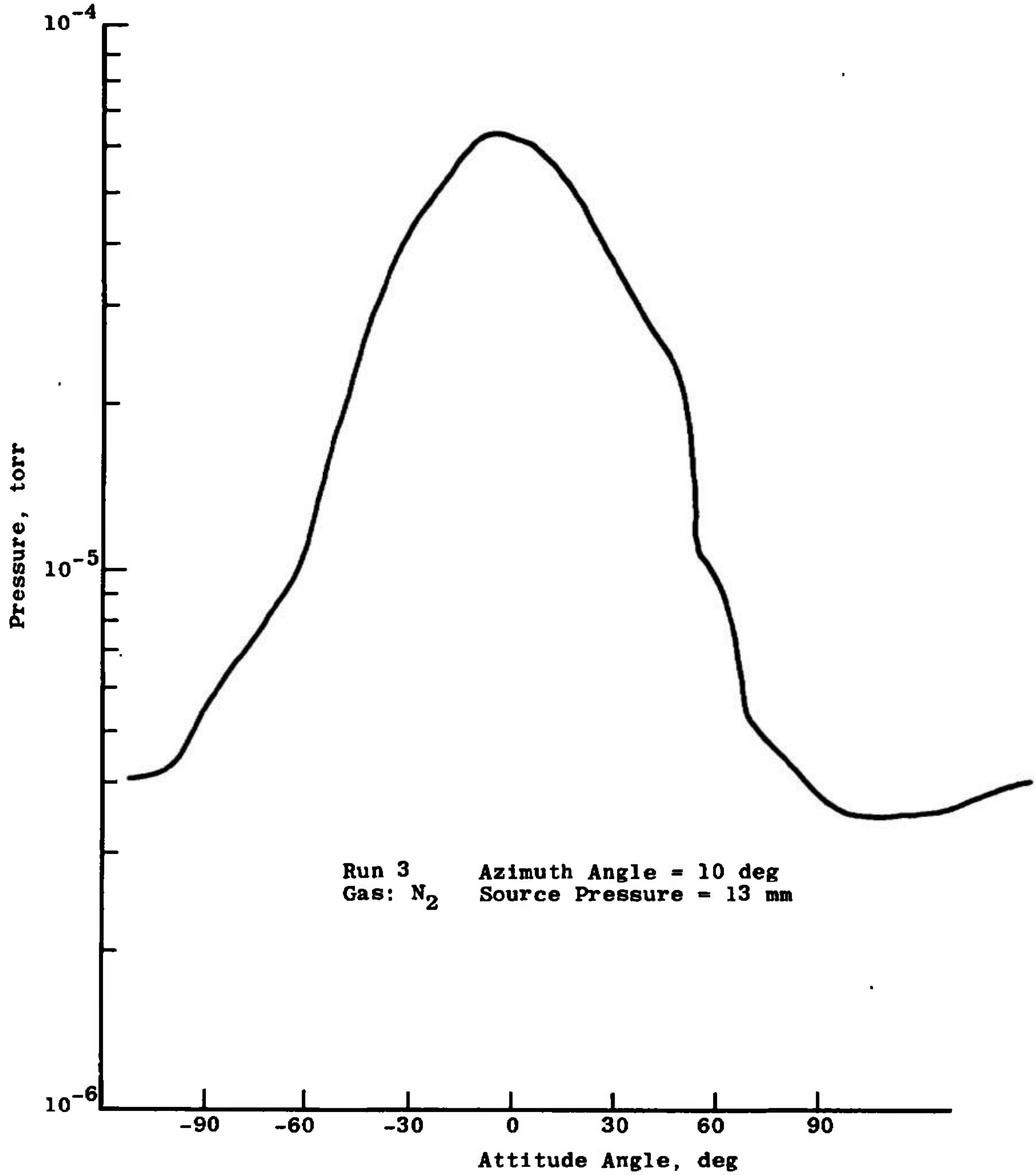


c. Run 3
Fig. 10 Continued

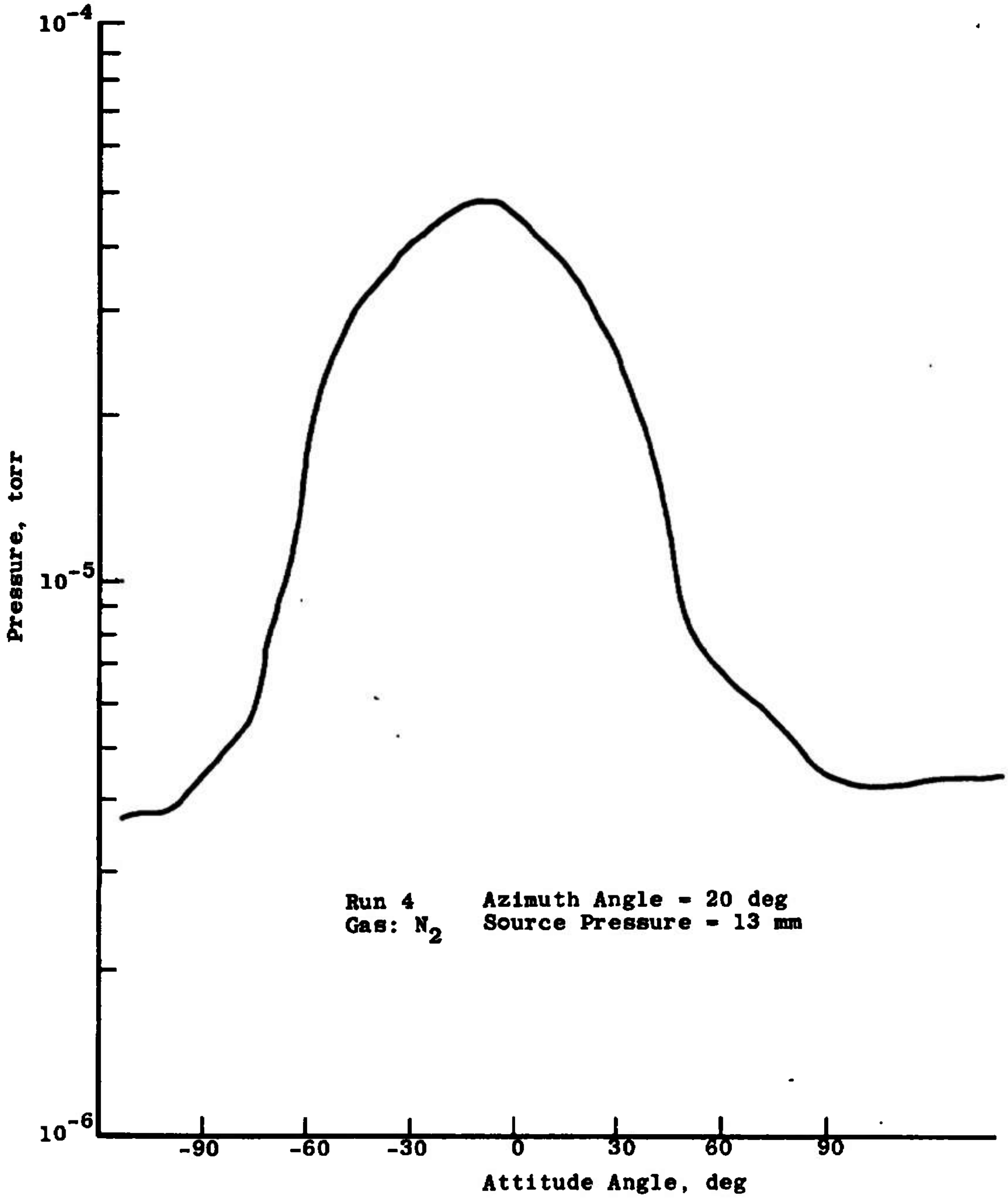


d. Run 4
Fig. 10 Continued

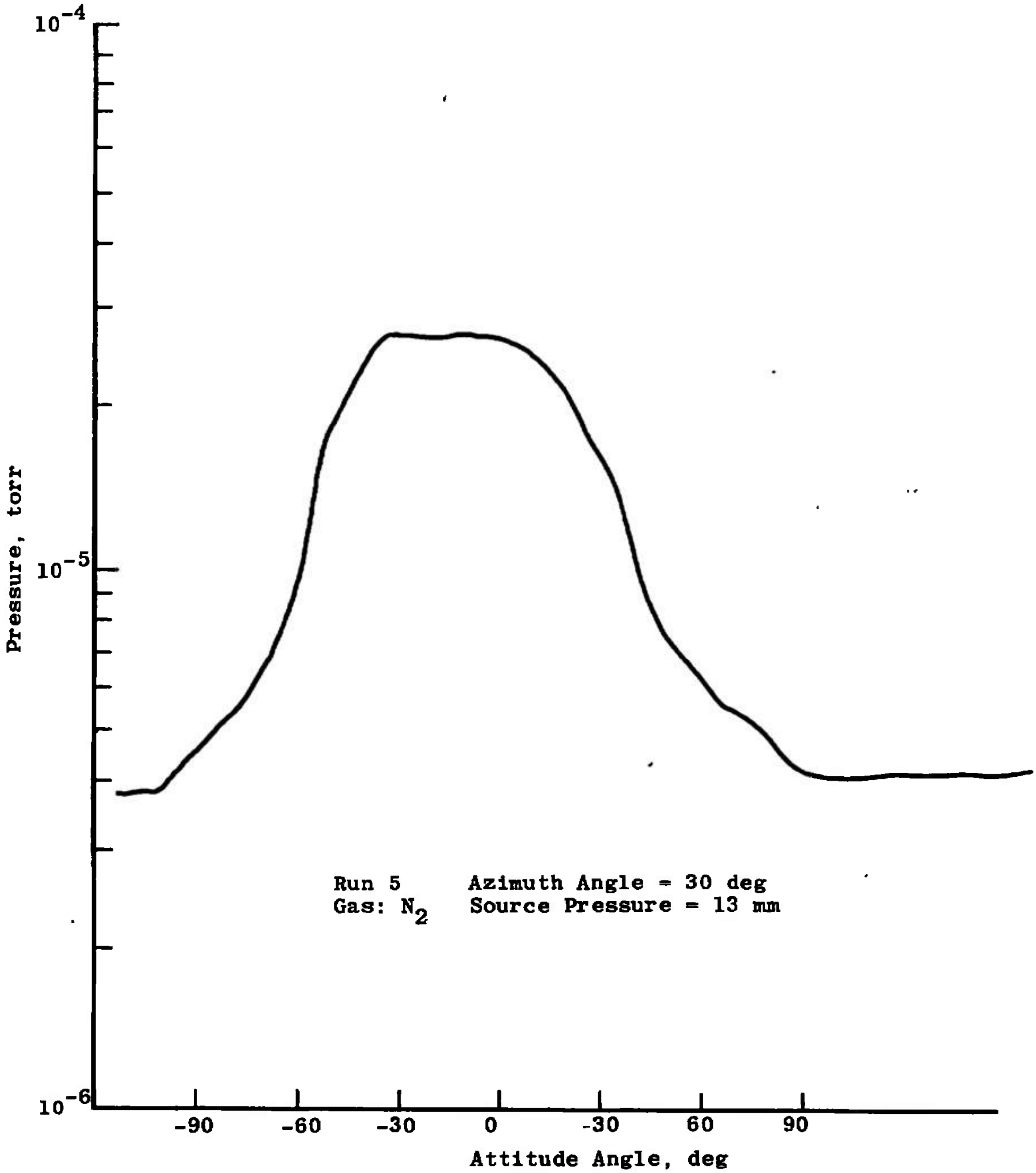


e. Run 5
Fig. 10 Continued

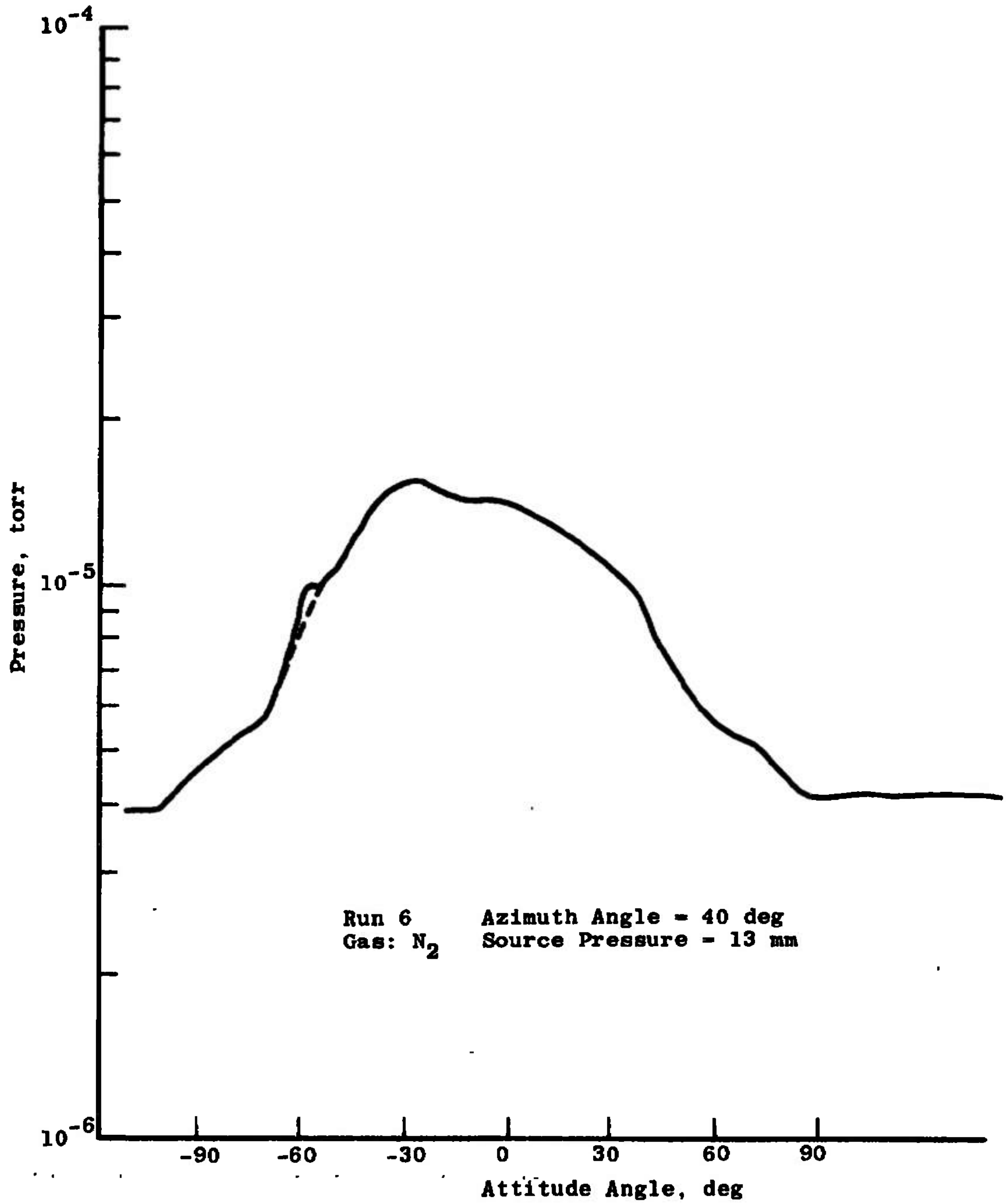


f. Run 6
Fig. 10 Continued

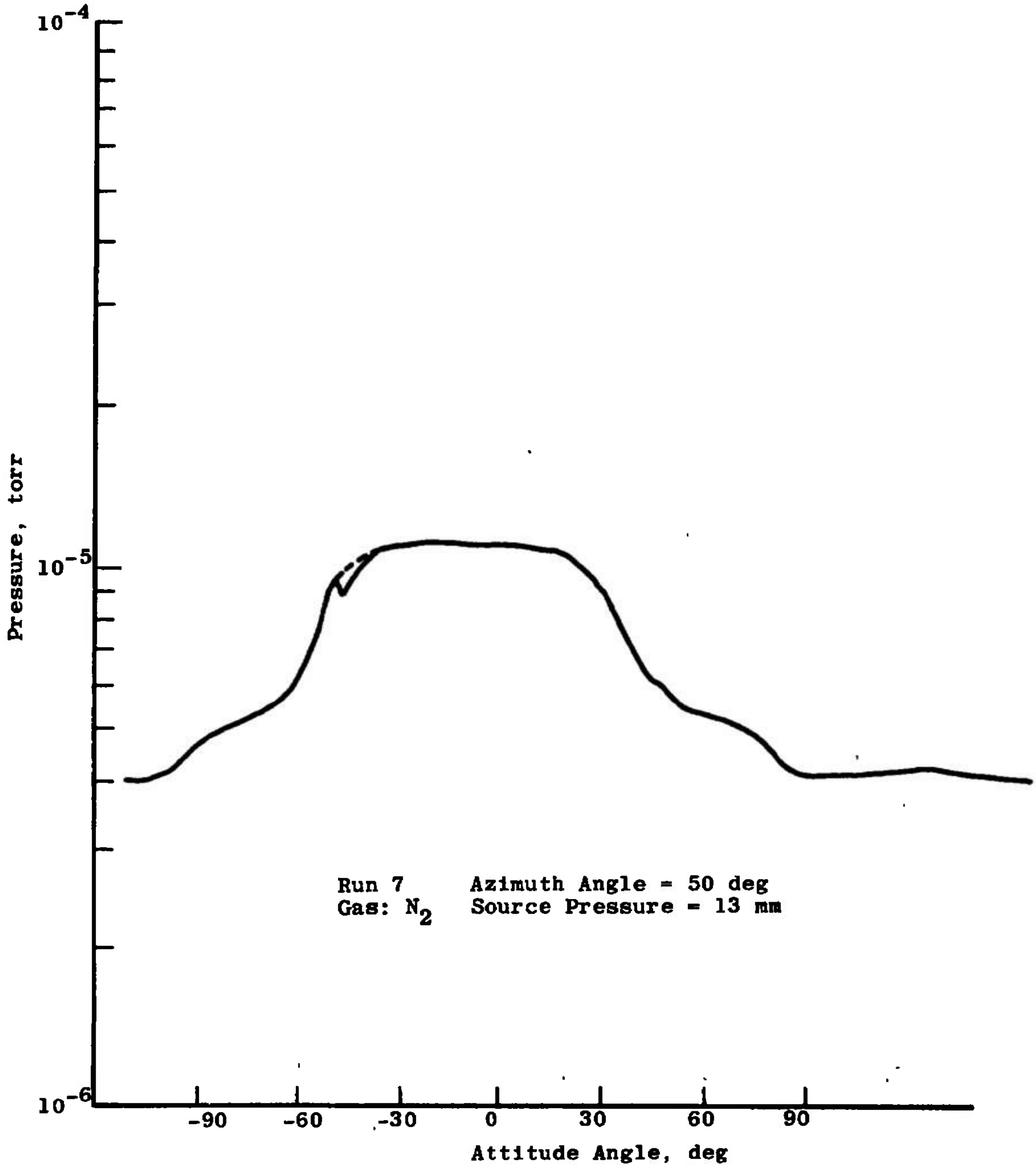


g. Run 7
Fig. 10 Continued

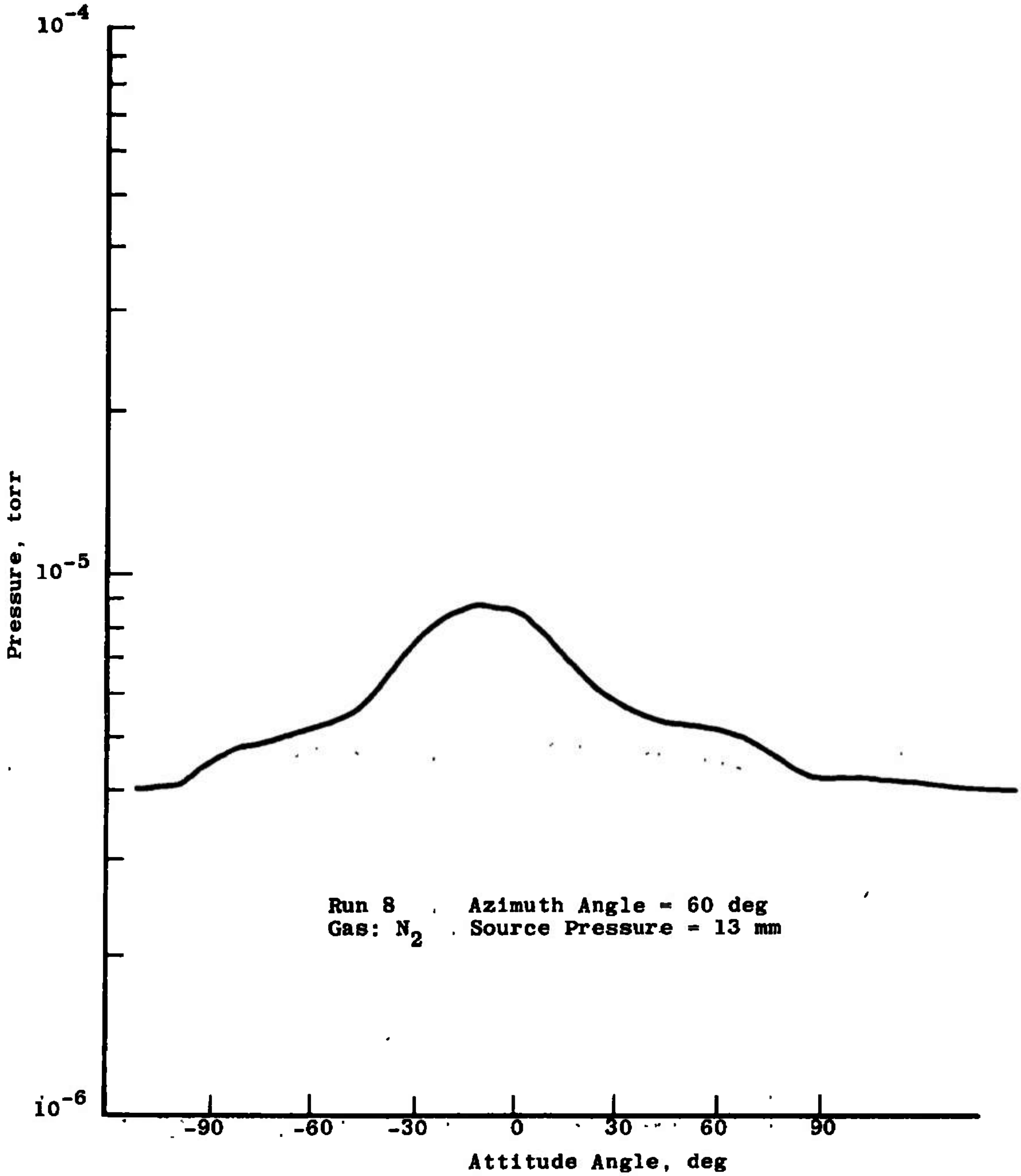


h. Run 8
Fig. 10 Continued

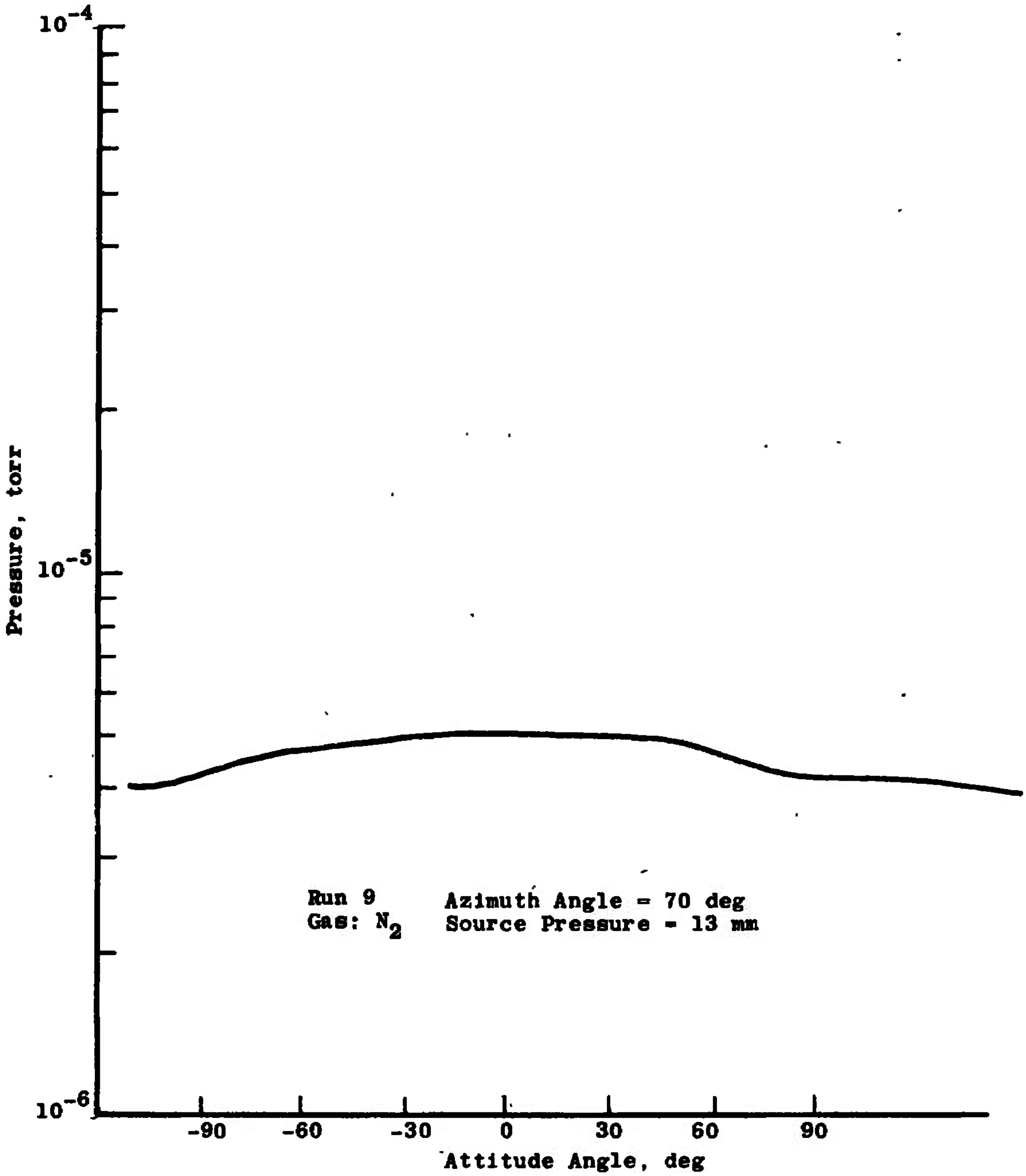


i. Run 9
Fig. 10 Continued

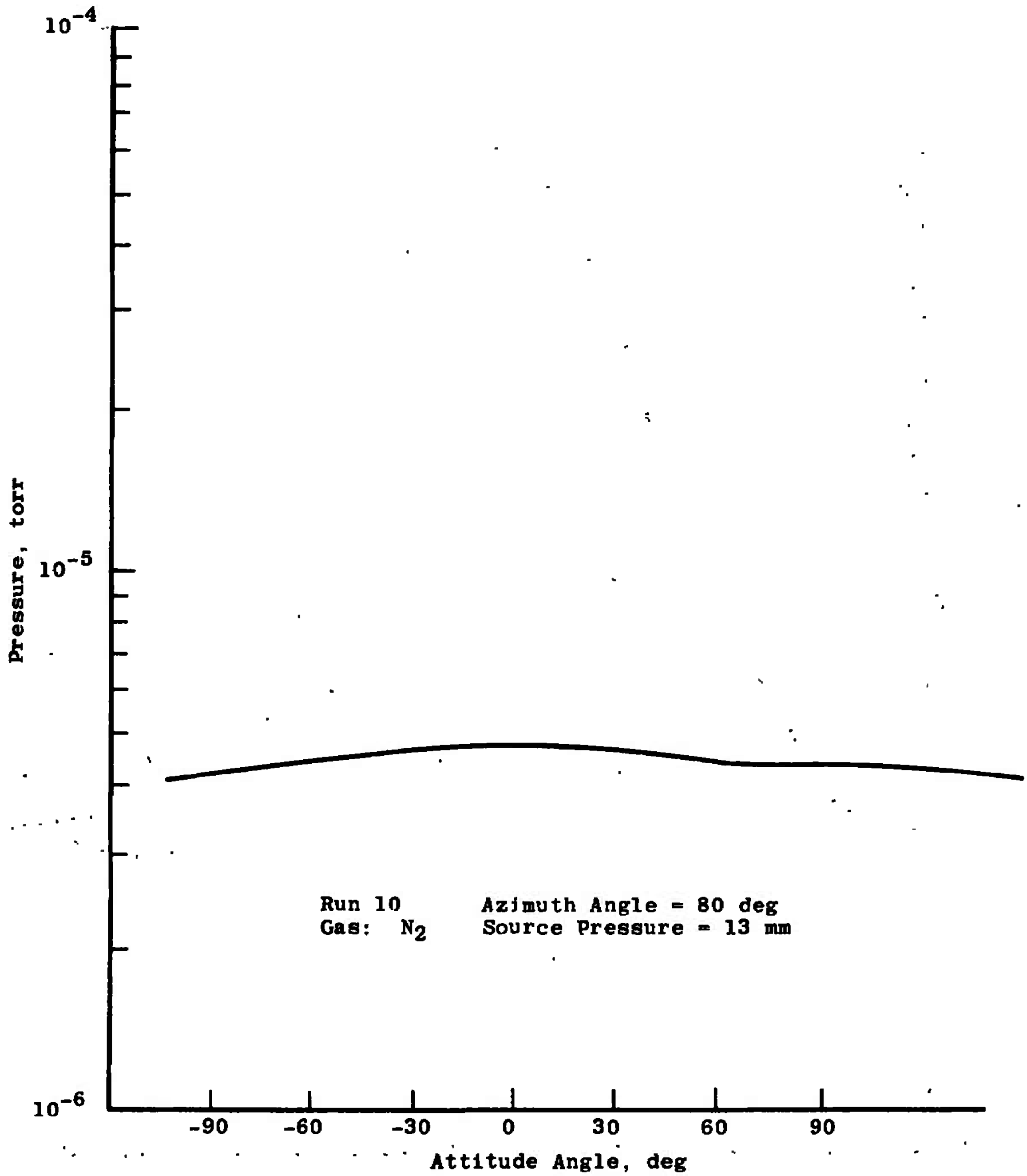


j. Run 10
Fig. 10 Continued

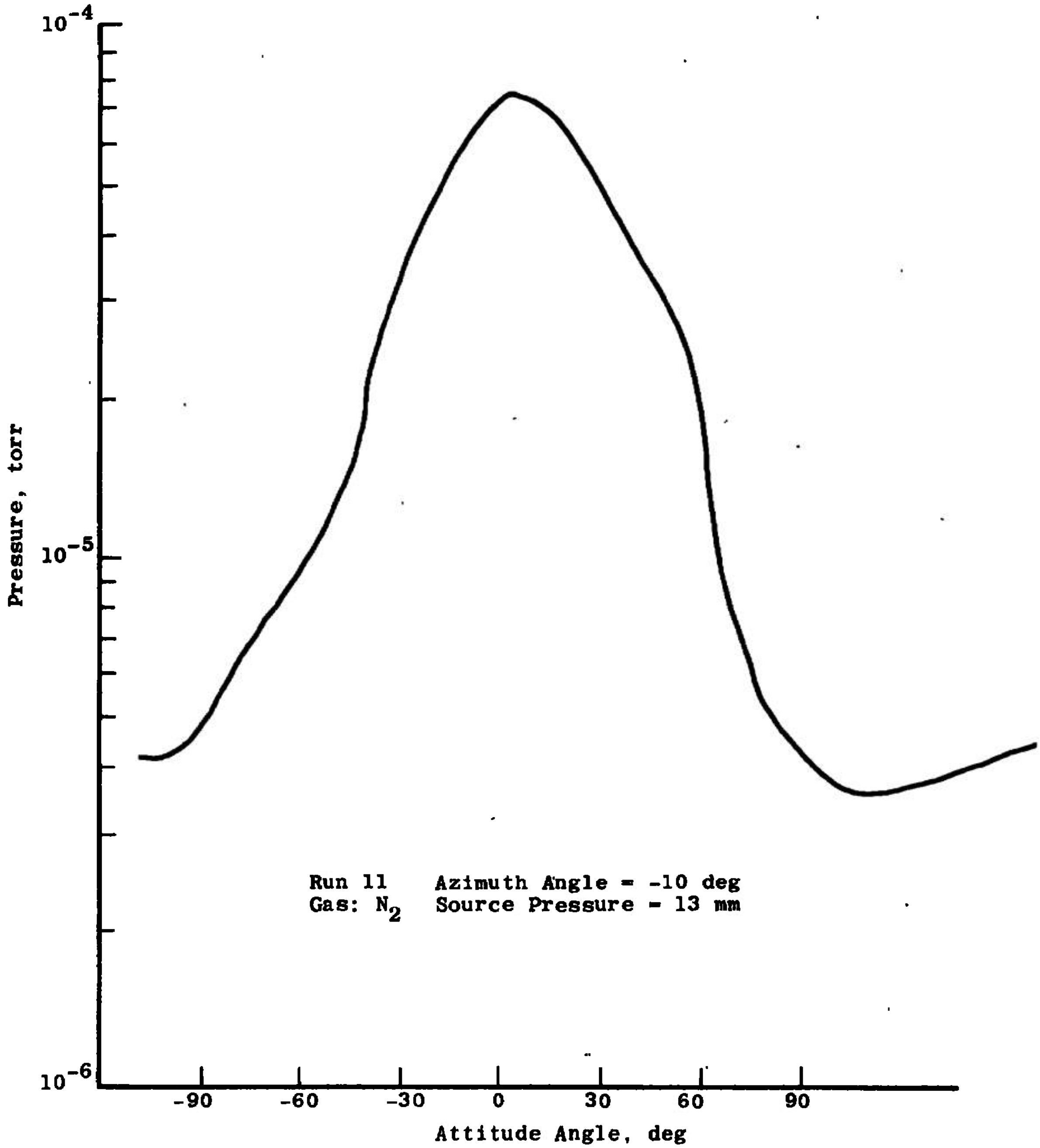


k. Run 11
Fig. 10 Continued

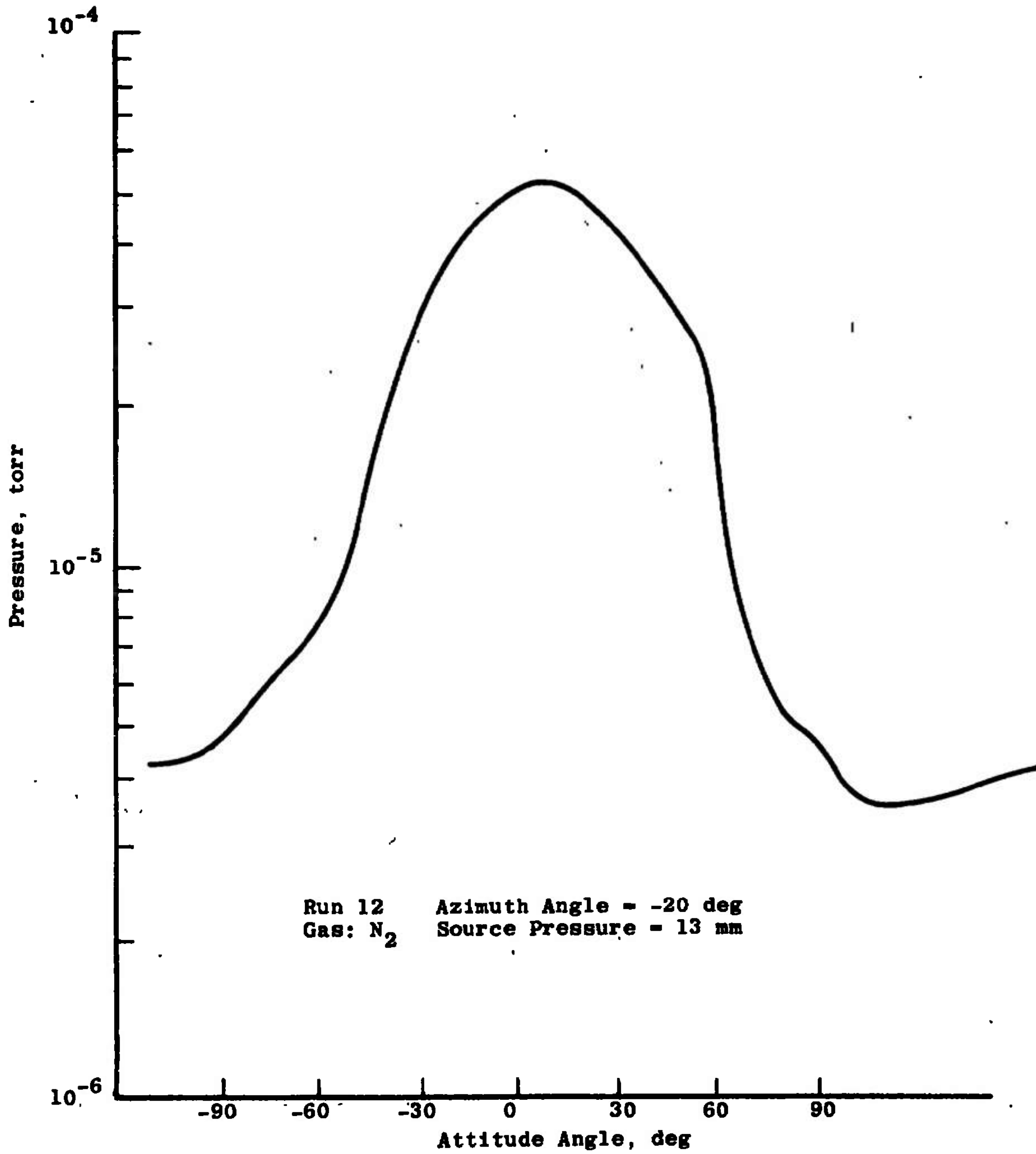


I. Run 12
Fig. 10 Continued

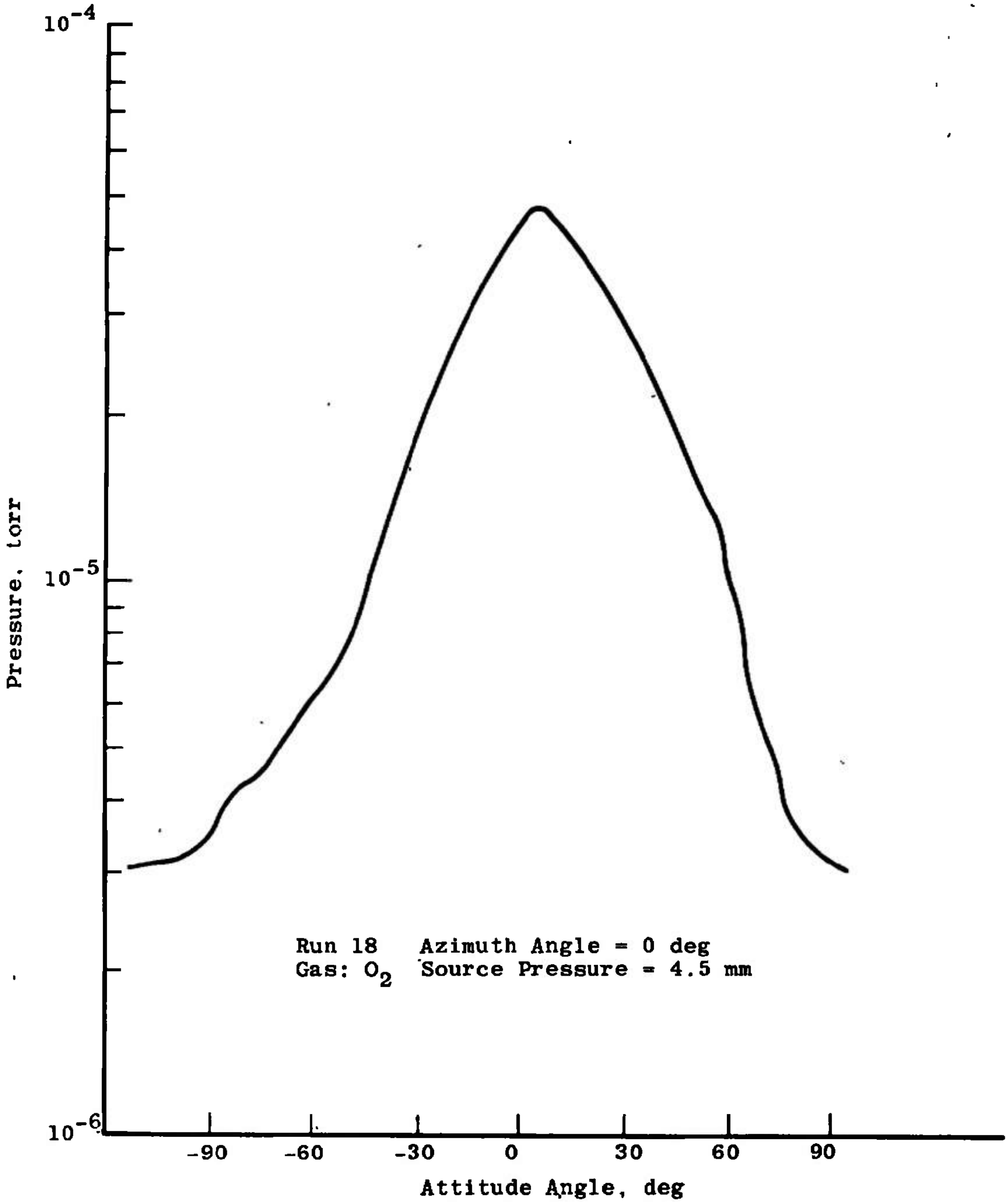


m. Run 18
Fig. 10 Continued

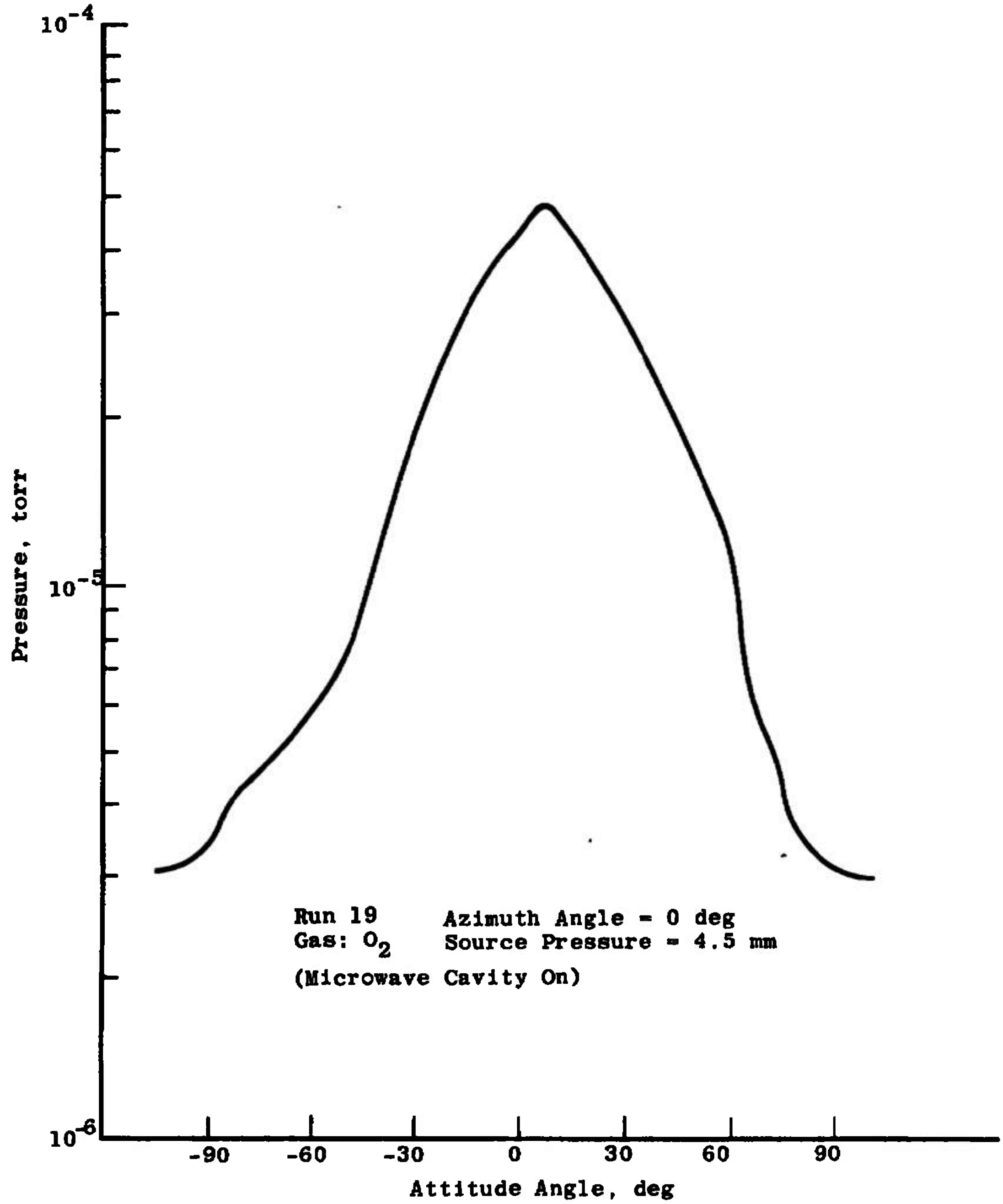


n. Run 19
Fig. 10 Continued

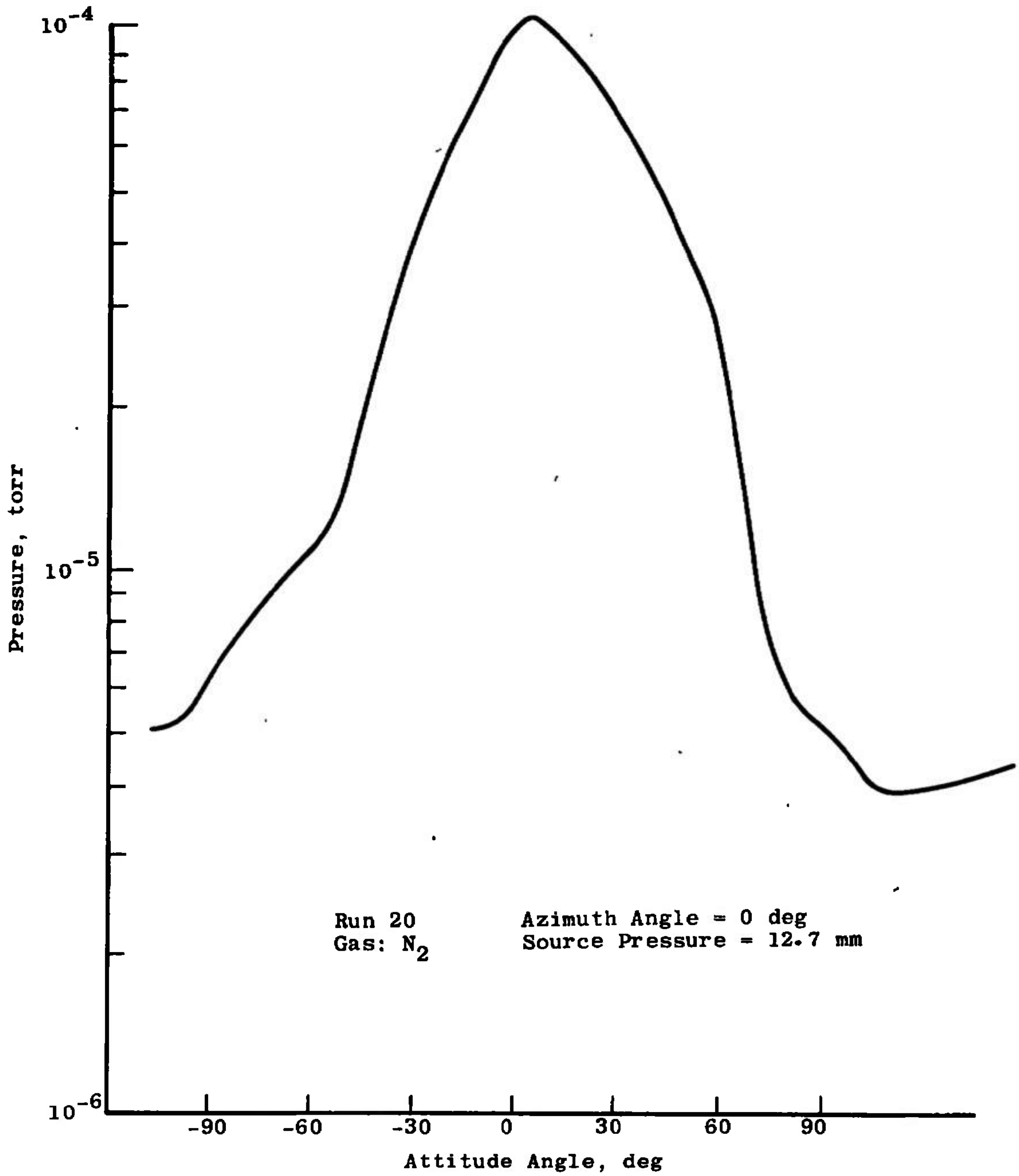


o. Run 20
Fig. 10 Concluded

| Azimuth, deg \ Elevation, deg | -90 | -80 | -70 | -60 | -50 | -40 | -30 | -20 | -10 | 0 | 10 | 20 | 30 | 40 | 50 | 60 | 70 | 80 | 90 | |
|---|---|---|---|---|---|---|---|---|---|---|---|---|---|---|---|---|---|---|---|---|
| -90 | | | | | | | | | | | | | | | | | | | | -90 |
| -80 | 0.04 | 0.04 | 0.04 | 0.04 | 0.04 | 0.04 | 0.04 | 0.04 | 0.04 | 0.04 | 0.04 | 0.04 | 0.04 | 0.04 | 0.04 | 0.04 | 0.04 | 0.04 | 0.03 | -80 |
| -70 | 0.03 | 0.04 | 0.04 | 0.04 | 0.04 | 0.04 | 0.04 | 0.04 | 0.04 | 0.04 | 0.04 | 0.04 | 0.04 | 0.04 | 0.04 | 0.04 | 0.04 | 0.04 | 0.03 | -70 |
| -60 | 0.03 | 0.04 | 0.04 | 0.04 | 0.04 | 0.04 | 0.05 | 0.05 | 0.06 | 0.07 | 0.07 | 0.07 | 0.07 | 0.06 | 0.05 | 0.04 | 0.04 | 0.04 | 0.04 | -60 |
| -50 | 0.03 | 0.04 | 0.04 | 0.04 | 0.05 | 0.05 | 0.06 | 0.10 | 0.11 | 0.11 | 0.11 | 0.11 | 0.11 | 0.11 | 0.09 | 0.05 | 0.04 | 0.04 | 0.03 | -50 |
| -40 | 0.04 | 0.04 | 0.04 | 0.05 | 0.06 | 0.09 | 0.11 | 0.13 | 0.14 | 0.15 | 0.15 | 0.16 | 0.16 | 0.14 | 0.11 | 0.07 | 0.05 | 0.04 | 0.03 | -40 |
| -30 | 0.04 | 0.04 | 0.05 | 0.05 | 0.06 | 0.09 | 0.17 | 0.22 | 0.26 | 0.28 | 0.29 | 0.29 | 0.29 | 0.25 | 0.16 | 0.09 | 0.05 | 0.04 | 0.03 | -30 |
| -20 | 0.04 | 0.04 | 0.05 | 0.06 | 0.06 | 0.12 | 0.20 | 0.30 | 0.39 | 0.45 | 0.48 | 0.46 | 0.40 | 0.35 | 0.30 | 0.09 | 0.09 | 0.04 | 0.03 | -20 |
| -10 | 0.04 | 0.04 | 0.05 | 0.07 | 0.08 | 0.12 | 0.27 | 0.38 | 0.53 | 0.59 | 0.64 | 0.61 | 0.53 | 0.41 | 0.32 | 0.20 | 0.09 | 0.05 | 0.03 | -10 |
| 0 | 0.04 | 0.05 | 0.06 | 0.09 | 0.13 | 0.22 | 0.35 | 0.51 | 0.67 | 0.83 ● | 0.91 | 0.74 | 0.59 | 0.46 | 0.38 | 0.22 | 0.07 | 0.05 | 0.04 | 0 |
| 10 | 0.04 | 0.04 | 0.05 | 0.07 | 0.08 | 0.12 | 0.27 | 0.38 | 0.53 | 0.59 | 0.64 | 0.61 | 0.53 | 0.41 | 0.32 | 0.20 | 0.09 | 0.05 | 0.03 | 10 |
| 20 | 0.04 | 0.04 | 0.05 | 0.06 | 0.06 | 0.12 | 0.20 | 0.30 | 0.39 | 0.45 | 0.48 | 0.46 | 0.40 | 0.35 | 0.30 | 0.09 | 0.05 | 0.04 | 0.03 | 20 |
| 30 | 0.04 | 0.04 | 0.05 | 0.05 | 0.06 | 0.09 | 0.17 | 0.22 | 0.26 | 0.28 | 0.29 | 0.29 | 0.29 | 0.25 | 0.16 | 0.09 | 0.05 | 0.04 | 0.03 | 30 |
| 40 | 0.04 | 0.04 | 0.04 | 0.05 | 0.06 | 0.09 | 0.11 | 0.13 | 0.14 | 0.15 | 0.15 | 0.16 | 0.16 | 0.14 | 0.11 | 0.07 | 0.05 | 0.04 | 0.03 | 40 |
| 50 | 0.03 | 0.04 | 0.04 | 0.04 | 0.05 | 0.05 | 0.06 | 0.10 | 0.11 | 0.11 | 0.11 | 0.11 | 0.11 | 0.11 | 0.09 | 0.05 | 0.04 | 0.04 | 0.03 | 50 |
| 60 | 0.03 | 0.04 | 0.04 | 0.04 | 0.04 | 0.04 | 0.05 | 0.05 | 0.06 | 0.07 | 0.07 | 0.07 | 0.07 | 0.06 | 0.05 | 0.04 | 0.04 | 0.04 | 0.04 | 60 |
| 70 | 0.03 | 0.04 | 0.04 | 0.04 | 0.04 | 0.04 | 0.04 | 0.04 | 0.04 | 0.04 | 0.04 | 0.04 | 0.04 | 0.04 | 0.04 | 0.04 | 0.04 | 0.04 | 0.03 | 70 |
| 80 | 0.04 | 0.04 | 0.04 | 0.04 | 0.04 | 0.04 | 0.04 | 0.04 | 0.04 | 0.04 | 0.04 | 0.04 | 0.04 | 0.04 | 0.04 | 0.04 | 0.04 | 0.04 | 0.03 | 80 |
| 90 | | | | | | | | | | | | | | | | | | | | 90 |
| | -90 | -80 | -70 | -60 | -50 | -40 | -30 | -20 | -10 | 0 | 10 | 20 | 30 | 40 | 50 | 60 | 70 | 80 | 90 | |

Elevation, deg

Fig. 11 Matrix of Correction Factors

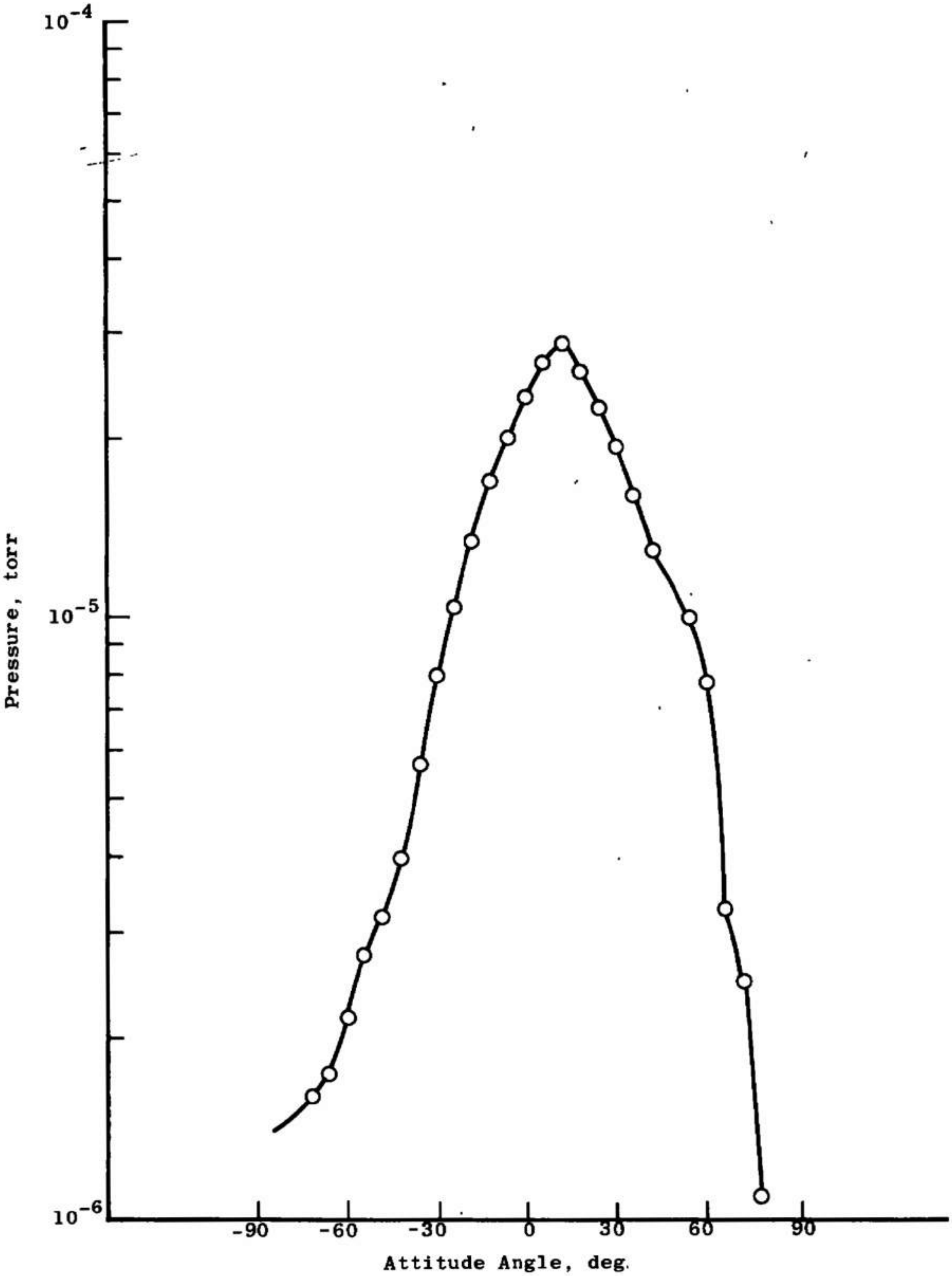


Fig. 12 Pressure Profile for Constant Azimuth

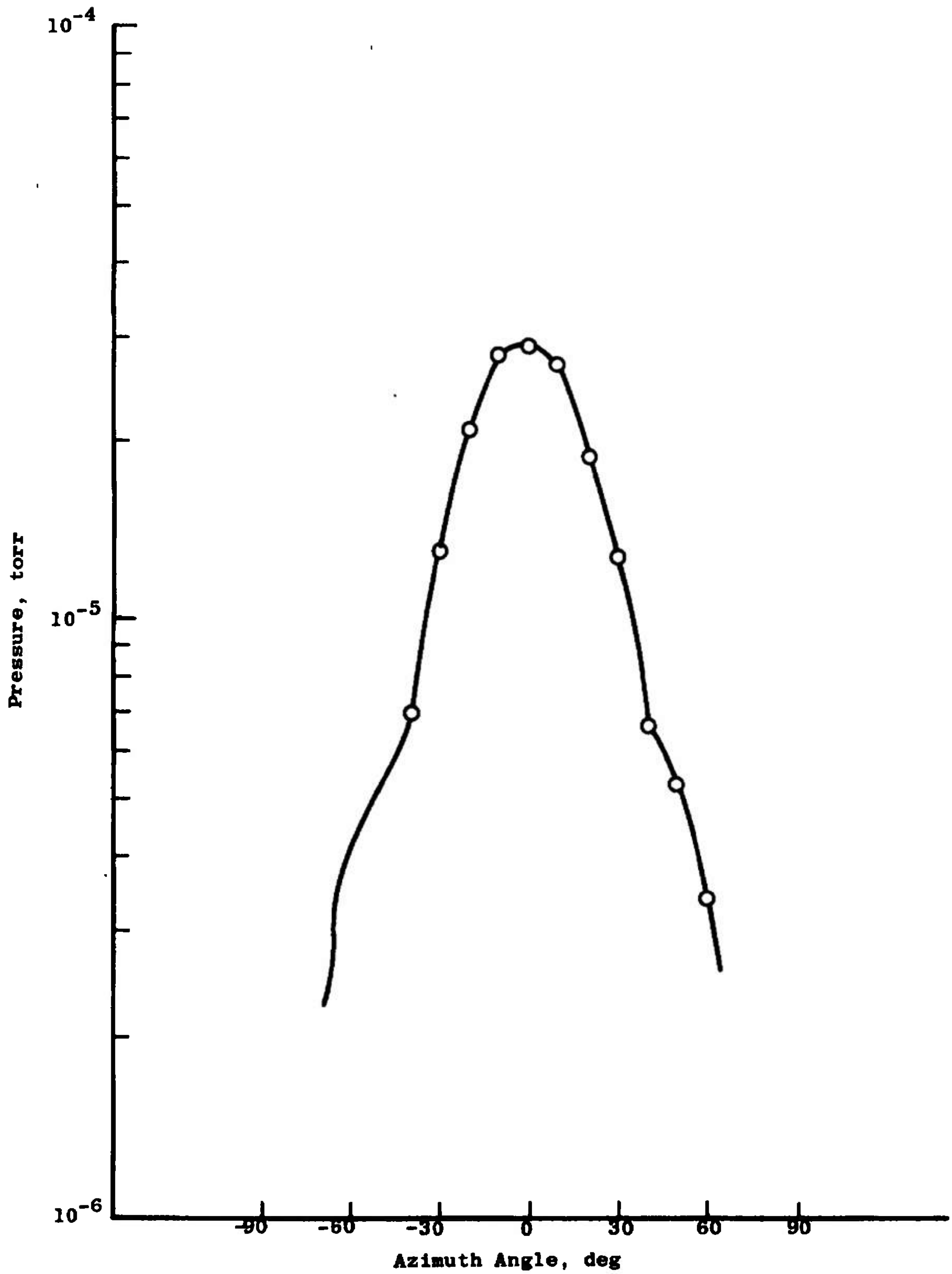


Fig. 13 Pressure Profile for Constant Attitude

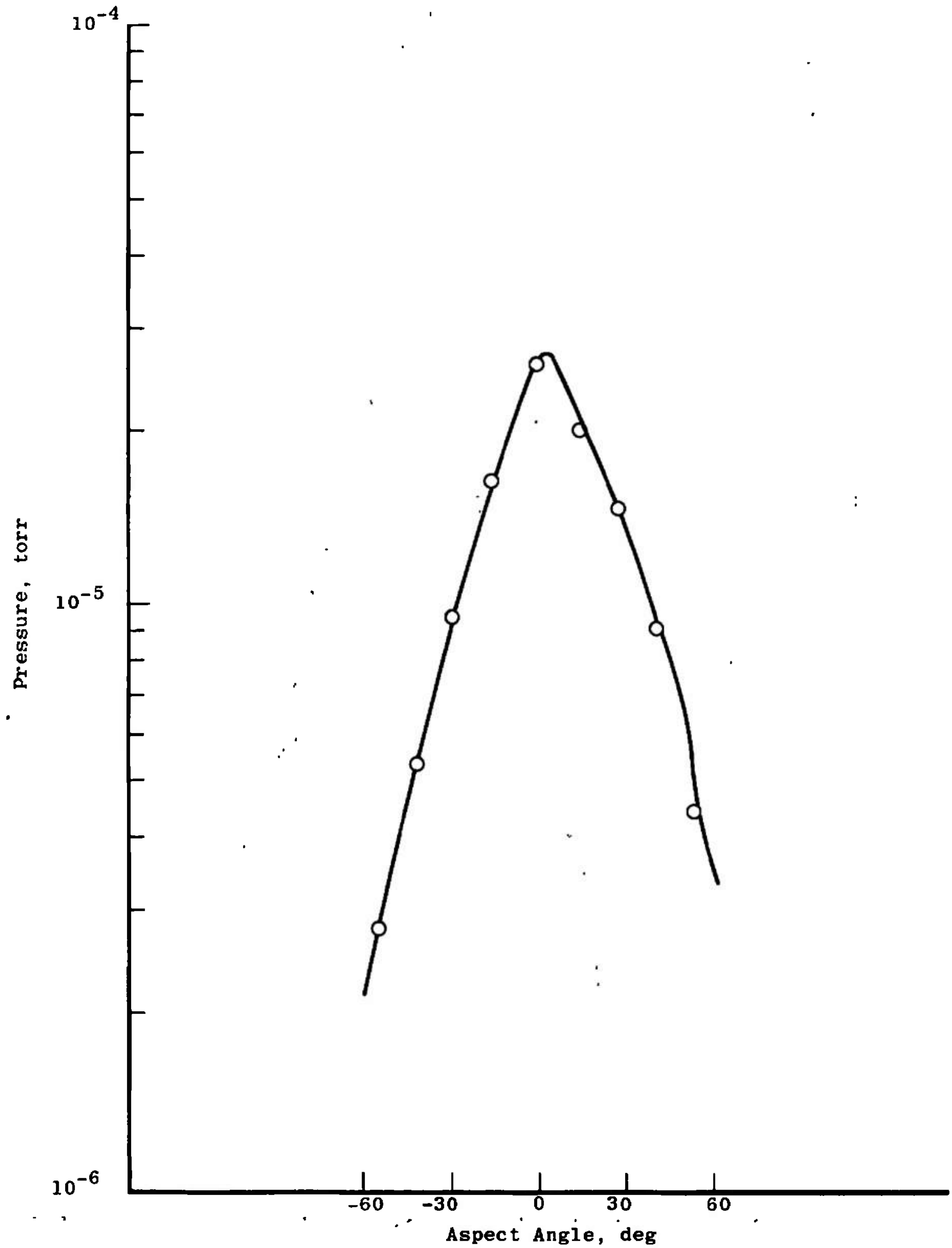


Fig. 14 Pressure Profile for Varying Azimuth and Attitude

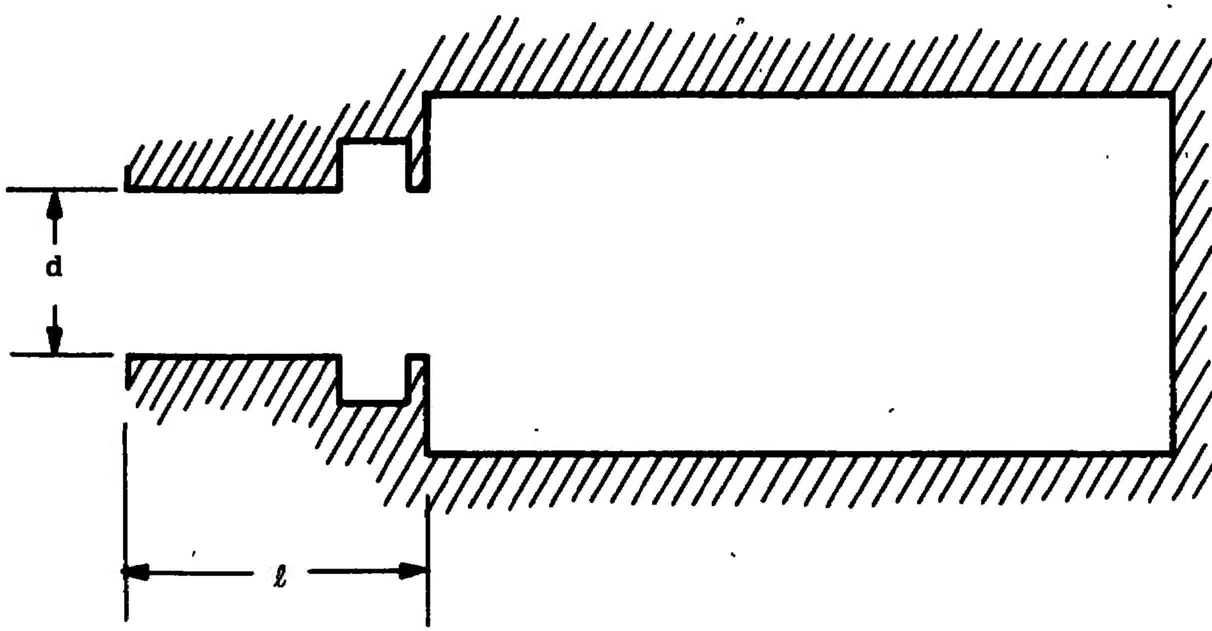


$D = d/\ell = 0.8$

Gage Tubulation

**Fig. 15 Schematic of CRL Gage**

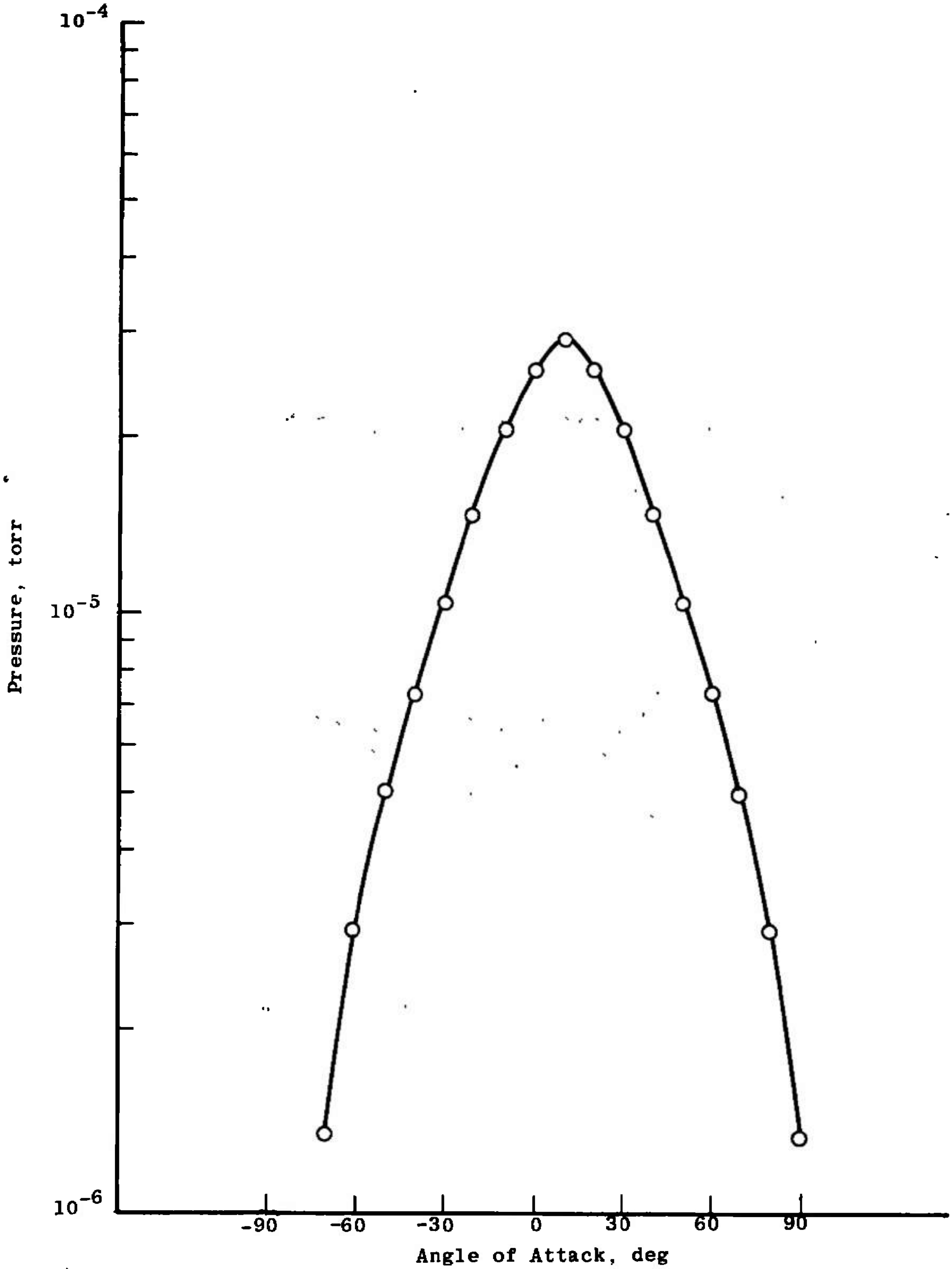


a. S = 10, D = 0.75
Fig. 16 Predicted Pressure Profiles

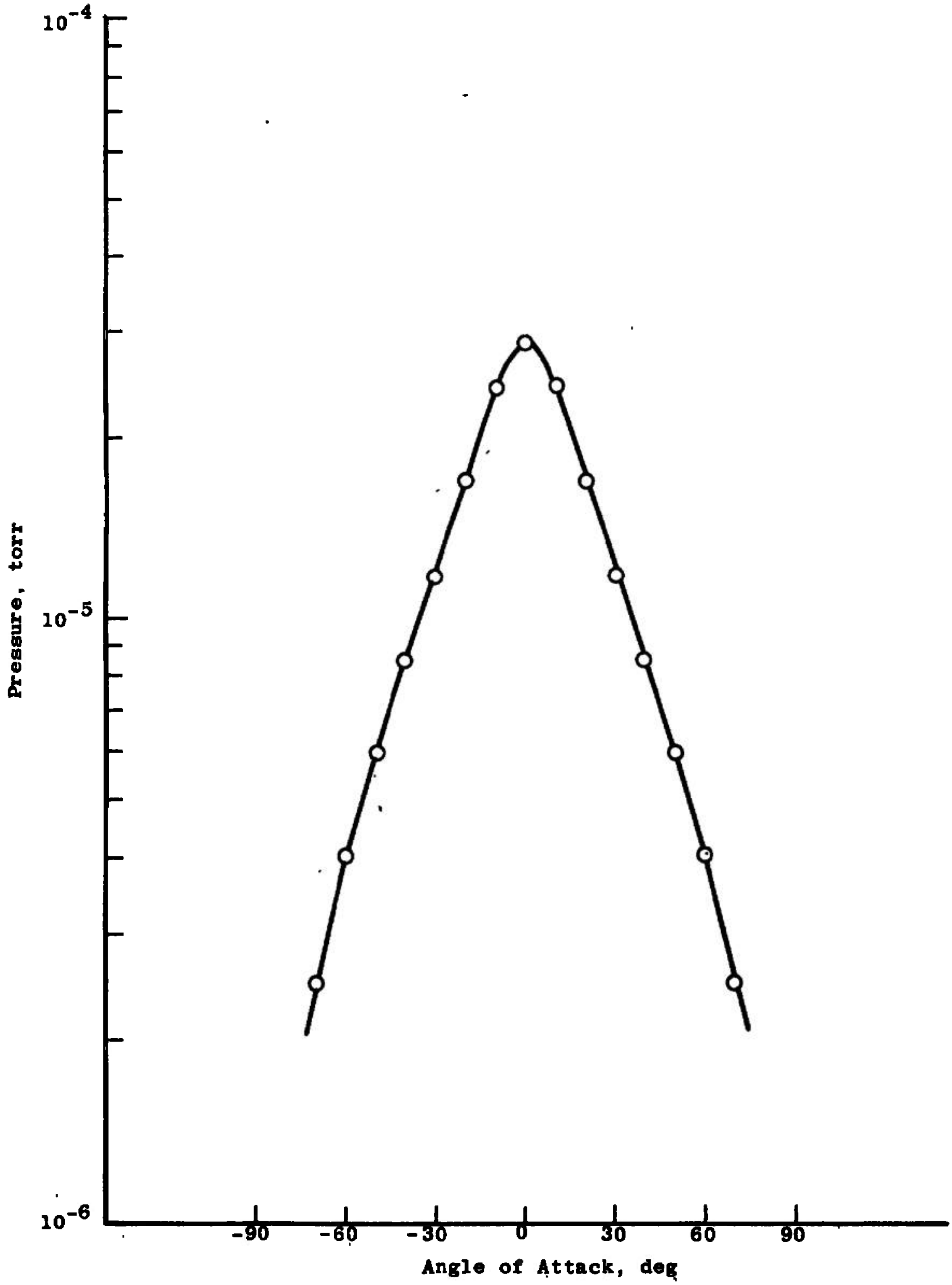


b. S = 10, D = 0.5
Fig. 16 Continued

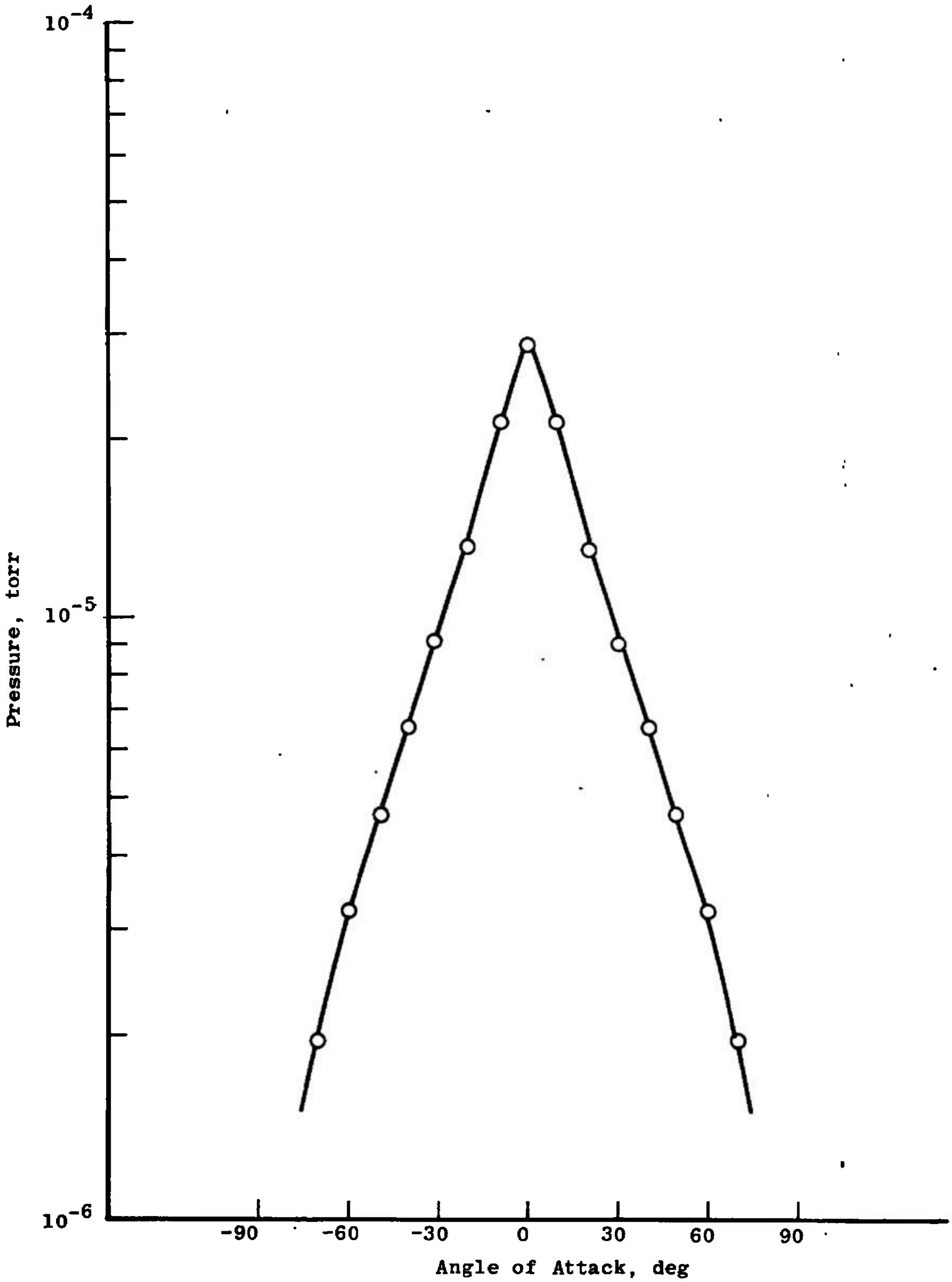


c. S = 10, D = 0.3
Fig. 16 Continued

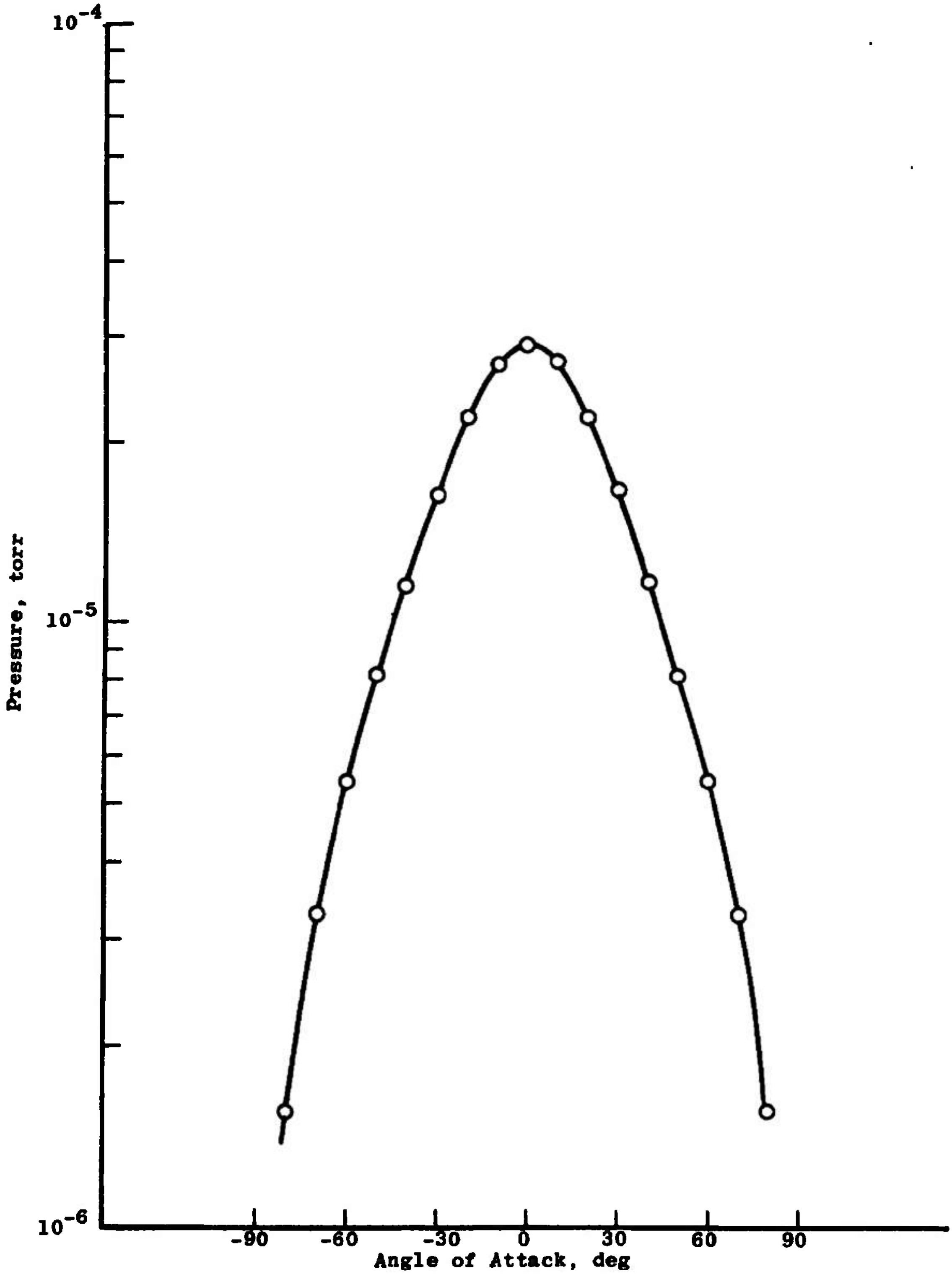


d. S = 5, D = 0.75
Fig. 16 Continued

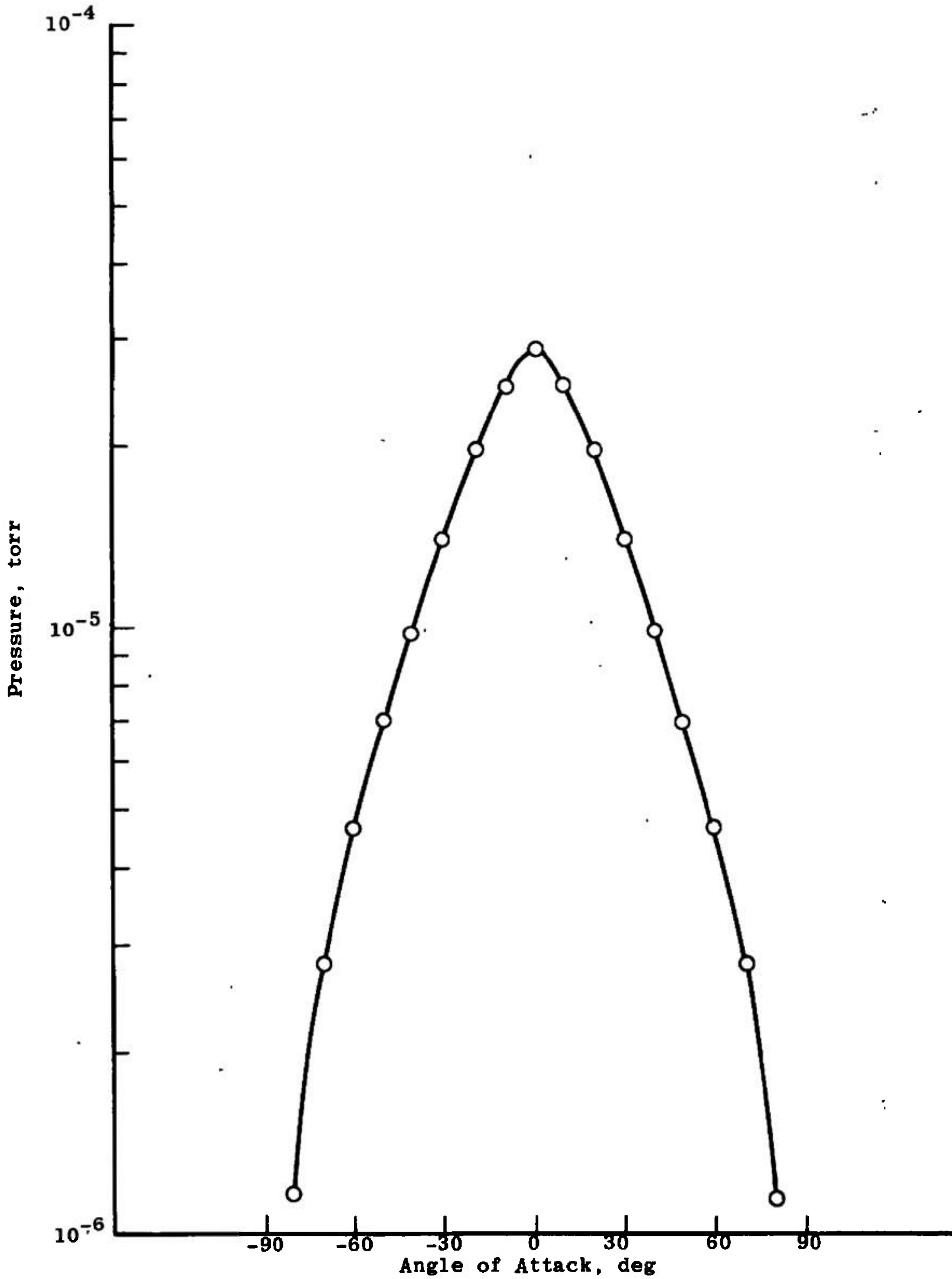


e. S = 20, D = 0.75
Fig. 16 Concluded

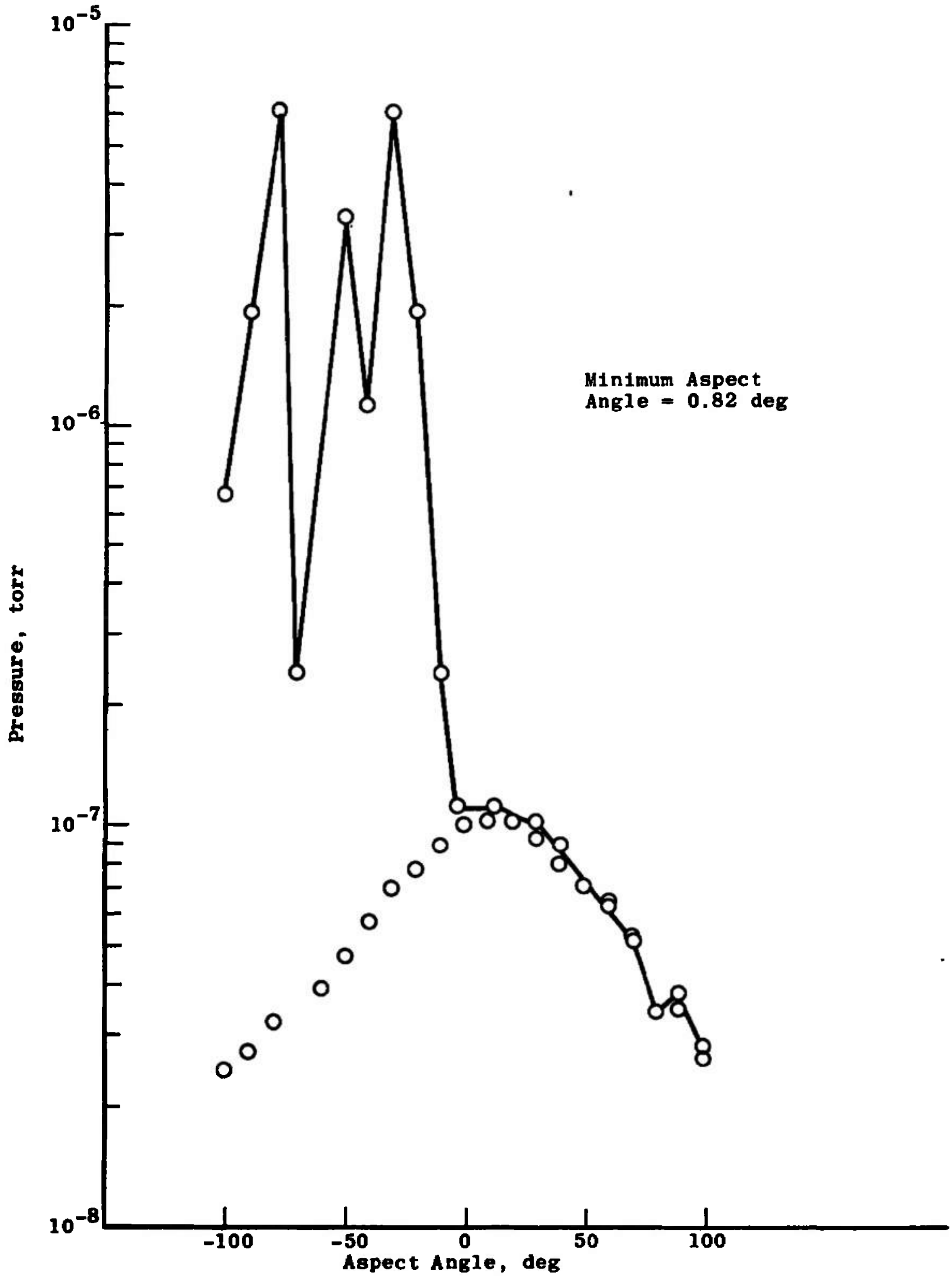


Fig. 17 Satellite Data Indicating Oscillations

**DOCUMENT CONTROL DATA - R & D**

*(Security classification of title, body of abstract and indexing annotation must be entered when the overall report is classified)*

| | |
|---|---|
| 1. ORIGINATING ACTIVITY *(Corporate author)*<br>Arnold Engineering Development Center<br>ARO, Inc., Operating Contractor<br>Arnold Air Force Station, Tennessee 37389 | 2a. REPORT SECURITY CLASSIFICATION<br>UNCLASSIFIED<br>2b. GROUP<br>N/A |

3. REPORT TITLE

EVALUATION OF A PRESSURE GAGE ROTATING IN A MOLECULAR FLUX

4. DESCRIPTIVE NOTES *(Type of report and inclusive dates)*

Final Report - July 1, 1969 to June 1970

5. AUTHOR(S) *(First name, middle initial, last name)*

J. D. Haygood and R. Dawbarn, ARO, Inc.

| 6. REPORT DATE | 7a. TOTAL NO. OF PAGES | 7b. NO. OF REFS |
|---|---|---|
| April 1971 | 66 | 6 |

| | |
|---|---|
| 8a. CONTRACT OR GRANT NO.<br>F40600-71-C-0002<br>b. PROJECT NO. 8605<br>c. Program Element 61102F<br>d. | 9a. ORIGINATOR'S REPORT NUMBER(S)<br>AEDC-TR-70-287<br>9b. OTHER REPORT NO(S) *(Any other numbers that may be assigned this report)*<br>ARO-VKF-TR-70-274 |

10. DISTRIBUTION STATEMENT

Approved for public release; distribution unlimited.

| 11. SUPPLEMENTARY NOTES | 12. SPONSORING MILITARY ACTIVITY |
|---|---|
| Available in DDC | Air Force Cambridge Research Lab, Air Force Systems Command, L. G. Hanscom Field, Bedford, Mass.01731 |

13. ABSTRACT

The purpose of this project was to help evaluate data obtained from an ion gage flown on board the OV1-15 satellite. The aerodynamic molecular beam facility was modified to produce a molecular beam with a 5-in.-diam test core. This system was used to determine the effects of a changing angle of attack on the pressure reading in a hot cathode magnetron ionization gage. Static calibrations were made for various orientations of the gage to the beam flow. Dynamic calibrations were made with the gage rotating in the beam flow at approximately 2 rpm. A comparison of static and dynamic profiles showed no detectable differences, thus indicating negligible sorption effects within the gage. The sensitivity factor for the gage was determined by calibrating the gage in a vacuum system where the random gas pressure could be controlled and set at known values. A matrix of correction factors was prepared which may be used to adjust the observed gage reading at a known attitude and azimuth angle to that pressure which would have been observed with the same molecular flux and the gage at 0-deg attitude and 0-deg azimuth.

| 14. KEY WORDS | LINK A | | LINK B | | LINK C | |
|---|---|---|---|---|---|---|
| | ROLE | WT | ROLE | WT | ROLE | WT |
| molecular beams | | | | | | |
| rarefied gas dynamics | | | | | | |
| pressure gages | | | | | | |
| ionization gages | | | | | | |
| sorption | | | | | | |
| atmospheric density | | | | | | |
| spacecraft | | | | | | |
| scientific satellites | | | | | | |

APSC
Arnold AFS Tenn